Modeling the Impact of Seasonality on Mosquito Population Dynamics: Insights for Vector Control Strategies

Joseph Baafi[1*] and Amy Hurford[1,2†]

[1]Department of Biology, Memorial University of Newfoundland, St. John's (NL), Canada, jbaafi@mun.ca, ahurford@mun.ca
[2]Department of Mathematics and Statistics, Memorial University of Newfoundland, St. John's (NL), Canada, ahurford@mun.ca

*Corresponding author's E-mail: jbaafi@mun.ca
Contributing author's E-mail: ahurford@mun.ca
† These authors contributed equally to this work.

Abstract

Mosquitoes are important vectors for the transmission of some major infectious diseases of humans, i.e., malaria, dengue, West Nile Virus and Zika virus. The burden of these diseases is different for different regions, being highest in tropical and subtropical areas, which have high annual rainfall, warm temperatures, and less pronounced seasonality. The life cycle of mosquitoes consists of four distinct stages: eggs, larvae, pupae, and adults. These life stages have different mortality rates and only adults can reproduce. Seasonal weather may affect the population dynamics of mosquitoes, and the relative abundance of different mosquito stages. We developed a stage-structured model that considers laboratory experiments describing how temperature and rainfall affects the reproduction, maturation and survival of different Anopheles mosquito stages, the species that transmits the parasite that causes malaria. We consider seasonal temperature and rainfall patterns and describe the stage-structured population dynamics of the Anopheles mosquito in Ain Mahbel, Algeria, Cape Town, South Africa, Nairobi, Kenya and Kumasi, Ghana. We find that neglecting seasonality leads to significant overestimation or underestimation of mosquito abundance. We find that depending on the region, mosquito abundance: peaks one, two or four times a year, periods of low abundance are predicted to occur for durations ranging from six months (Ain Mahbel) to not at all (Nairobi); and seasonal patterns of relative abundance of stages are substantially different. The region with warmer temperatures and higher rainfall across the year, Kumasi, Ghana, is predicted to have higher mosquito abundance, which is broadly consistent with reported malaria deaths relative to the other countries considered by our study. Our analysis reveals distinct patterns in mosquito abundance across different months and regions. Control strategies often target one specific life stage, for example, applying larvicides to kill mosquito larvae, or spraying insecticides to kill adult mosquitoes. Our findings suggest that differences in seasonal weather affect mosquito stage structure, and that the best approaches to vector control may differ between regions in timing, duration, and efficacy.

Keywords: Seasonality, mosquitoes, population dynamics, stage-structure, *anopheles* species, vector control.

1 Introduction

Mosquito-borne diseases continue to pose a significant global threat to human health, particularly in tropical and subtropical regions [1, 2, 3]. Malaria, dengue fever, Zika virus, and various other diseases transmitted by vectors impose a significant burden on communities around the globe [4, 5, 6]. Among the vectors responsible for transmitting these diseases, *Anopheles* mosquitoes are of paramount concern due to their role in spreading malaria, which affects millions of people worldwide. Approximately half of the global population is at risk of malaria [1, 7, 8]. Certain parts of the world have successfully eliminated malaria and have been certified malaria-free by WHO (for example, Mauritius in 1973, Morocco in 2010, Croatia in 1973, and Argentina in 2019) [9], malaria remains a persistent threat, even in countries with temperate climates, such as the United States, where recent malaria cases have been reported [2]. In 2021, a staggering 247 million cases of malaria were reported in 85 countries, resulting in over 619,000 deaths [1]. A significant majority of these cases occurred in sub-Saharan Africa, with the region accounting for 96% of malaria-related deaths and 95% of malaria cases in 2021 [2]. To control disease spread, it may be necessary to control vector populations in disease-endemic regions. Population dynamics vary regionally and best approaches to vector management, such as mosquitoes, are likely region-specific [10, 11].

Weather conditions, including temperature, precipitation, and humidity, have long been recognized as pivotal determinants influencing mosquito life cycles, population abundance, and the dynamics of disease transmission [12, 13, 14, 15, 16, 17, 3]. The diverse climates and regions across the globe give rise to distinct ecosystems, introducing variability that can impact both mosquito populations and their stage structure. Recent studies have made significant strides by incorporating temperature dependencies into models, accounting for factors such as egg oviposition, mortality, and maturation rates, thus enhancing the predictability of mosquito population dynamics, as demonstrated in studies focusing on *Culex pipiens* [18, 12]. Models that consider temperature dependence have exhibited robust performance across various species within specific regions [19, 20, 21, 12]. The success of these models underscores the importance of investigating the relationship between regional weather variability and mosquito dynamics. Mathematical models that neglect seasonal variations offer simplicity in analysis but may produce inaccurate outcomes and fail to provide adequate insights for determining optimal timing for implementing control measures [22, 11] during different periods of the year.

Various models have been developed to assess the impact of seasonality in environmental conditions on the transmission dynamics of mosquito-borne diseases such as malaria [23, 14] and dengue [17, 24, 20, 25]. Some of these models have delved into mosquito population dynamics under seasonal weather conditions using ordinary differential equation formulations [26, 21, 13, 27, 12] or delay-differential equation systems [28, 29]. However, the majority of existing models are tailored to specific mosquito species within particular geographic contexts. For instance, models have been developed for *Aedes aegypti*, in Brazil [20, 25]; *Anopheles gambiae* in the Sahel region of Africa [30]; *Anopheles arabiensis* in Zambia [31]; *Anopheles arabiensis* in KwaZulu-Natal, South Africa [21] and *Culex* in the Peel Region, Canada [19, 12]). Nonetheless, the generalizability of mosquito population estimates

and recommendations for vector control derived from these models may be constrained by variations in regional seasonality and adaptive traits. Despite some studies investigating the impacts of regional seasonality on mosquito population dynamics [32], further investigation in this area is warranted.

For this study, we focus on four distinct regions in Africa: Algeria, South Africa, Kenya, and Ghana. Each region presents a unique climate and ecological context, allowing us to investigate how the interplay of temperature and rainfall influences mosquito population dynamics and stage structure. This study has dual primary objectives. Firstly, we aim to gain a comprehensive understanding of how regional seasonality influences mosquito population dynamics. The integration of temperature and rainfall data into our stage-structured model allows us to assess the impact of these weather variables on mosquito survival, developmental rates, and population growth throughout different seasons. Secondly, we will try to derive insights that can inform effective vector control strategies. By exploring the intricate relationship between environmental conditions and mosquito population dynamics, we can pinpoint periods of peak mosquito abundance. This knowledge enables us to strategically implement interventions during these critical time frames.

The insights obtained from this study hold significance for public health authorities and researchers, guiding the development of context-specific strategies to mitigate mosquito-borne diseases. Potential strategies may include optimizing the timing of insecticide applications, implementing targeted larval source reduction measures, and enhancing surveillance systems to promptly detect and respond to periods of elevated mosquito abundance. This research aims to contribute actionable knowledge, paving the way for more targeted and efficient mosquito control interventions.

The paper is organized as follows: In section 2, we formulate the model and discuss the data used to find parameter estimates and parameter functions. Section 3 contains numerical simulations and results of the model discussed in section 2.1 using the temperature and rainfall data of four African regions. In section 4, we discuss the results and their implications and suggest possible future directions. The concluding remarks are presented in Section 5, summarizing key findings and contributions.

2 Methods

2.1 Model formulation

Mosquitoes progress through four distinct life stages: egg, larva, pupa, and adult. The first three stages occur in water, while the adult mosquitoes inhabit land and air [33, 34, 35]. The process begins with egg hatching, leading to the emergence of the first larval instar. Subsequently, the larva undergoes three additional molts, transitioning to the second, third, and fourth larval instars. After completing these stages, pupation occurs, giving rise to the pupa. Finally, the pupa undergoes metamorphosis, leading to the emergence of adult mosquitoes, both male and female. For successful reproduction, mating between male and female mosquitoes is necessary. Copulation results in the fertilization of the female, followed by the oviposition phase, where the adult female lays her eggs after obtaining a sufficient blood meal [29, 36, 37].

We formulate and analyze a stage-structured ordinary differential equation model that reflects details of the mosquito life cycle (Figure 1) and considers seasonal environment

(temperature- and rainfall-dependent). The stage structuring corresponds to the three main immature mosquito life stages: egg, $E(t)$; larva, $L(t)$; pupa, $P(t)$, and the adult female mosquitoes, $A_M(t)$. We incorporate stage-specific life history rates and processes to describe the rate of transitions between the life stages [28]. We split the adult stage into three sub-stages: adult seeking host, $A_h(t)$, adult at rest, $A_r(t)$ and ovipositing adult, $A_o(t)$ so that $A_M(t) = A_h(t) + A_r(t) + A_o(t)$. The model does not explicitly account for adult males but assumes their abundance to be equal to that of adult females. The model is given by the following deterministic system of nonlinear ordinary differential equations (ODE) 2.1.

$$\begin{aligned}
\frac{dE}{dt} &= b\phi_{A_0}(T)\left(1-\frac{A_o}{K}\right)A_0 - \left(\rho_E(T,R)+\mu_E(T)\right)E,\\
\frac{dL}{dt} &= \rho_E(T,R)E - \left(\rho_L(T,R)+\mu_L(T)+\sigma_L L\right)L,\\
\frac{dP}{dt} &= \rho_L(T,R)L - \left(\rho_P(T,R)+\mu_P(T)\right)P,\\
\frac{dA_h}{dt} &= \rho_P(T,R)P + \phi_{A_o}(T)A_o - \left(\rho_{A_h}+\mu_A(T)+\mu_{A_h}\right)A_h,\\
\frac{dA_r}{dt} &= \rho_{A_h}A_h - \left(\rho_{A_r}+\mu_A(T)\right)A_r,\\
\frac{dA_o}{dt} &= \rho_{A_r}A_r - \left(\phi_{A_o}(T)+\mu_A(T)+\mu_{A_o}\right)A_o,
\end{aligned} \tag{2.1}$$

with initial conditions $E(0), L(0), P(0), A_h(0), A_r(0)$ and $A_o(0)$. In system 2.1, $T = T(t)$ and $R = R(t)$ represent temperature and rainfall at time t, respectively. We assume that juvenile and adult mosquitoes experience the same temperature (that is, ambient and water temperatures are equivalent near the surface of the water) [12, 28]. Typically, sinusoidal functions, such as

$$T(t) = a + b_1 \sin\left(\frac{2\pi t}{365}\right) + b_2 \cos\left(\frac{2\pi t}{365}\right), \tag{2.2}$$

or

$$T(t) = T_0\left[1 + T_1 \cos\left(\frac{2\pi}{365}(\omega t + \theta)\right)\right], \tag{2.3}$$

are used to represent regional temperature fluctuations. Similar functions are used to account for rainfall variability (See figure 2). We assume that the functions $T(t)$ are non-negative, continuous, and bounded periodic functions. Also, the parameters $\phi_{A_0}(T)$, $\rho_E(T,R)$, $\rho_L(T,R)$, $\rho_P(T,R)$, $\mu_E(T)$, $\mu_L(T)$, $\mu_P(T)$ and $\mu_A(T)$ are non-negative, periodic, continuous and bounded functions defined on $[0,\infty)$.

The terms in each ordinary differential equation (ODE) in system 2.1 correspond to the rate of entry into a stage through the laying or hatching of eggs or maturation and the rate

of loss due to maturation and mortality. For further details about the model formulation see Appendix A.1, and for the definition of all variables and parameters see table 1.

The model 2.1 assumes density-dependent mortality of larvae, accounting for intra- and inter-species larval competition for resources (nutrients) and space (other studies have incorporated density-dependent larval mortality in their models including [12, 26, 32]). A flow diagram of the model 2.1 is shown in figure 1

The model 2.1 is used to understand mosquito stage structure and provide estimates for mosquito abundance due to variability in regional temperature and rainfall. It is an extension of the mosquito population model in Hamdan & Kilicman, (2010) [17], by adding: (i) the effect of temperature and rainfall, (ii) the aquatic stages of the mosquito explicitly, and (iii) density-dependent larval mortality rate. It also extends the non-autonomous mosquito dynamics model in Cailly et al.(2012) [13] and Abdelrazec & Gumel, (2017) [12] by giving a formulation of the temperature- and rainfall-dependent parameters of the model and by incorporating three female adult mosquito stages A_h, A_r, A_o to provide more accurate population estimates. We employ experimental data to parameterize temperature-dependent functions [28, 38, 39]. The functional expressions for rainfall-dependent parameters are extrapolated from the findings in [40], as also utilized in the investigation outlined in [32].

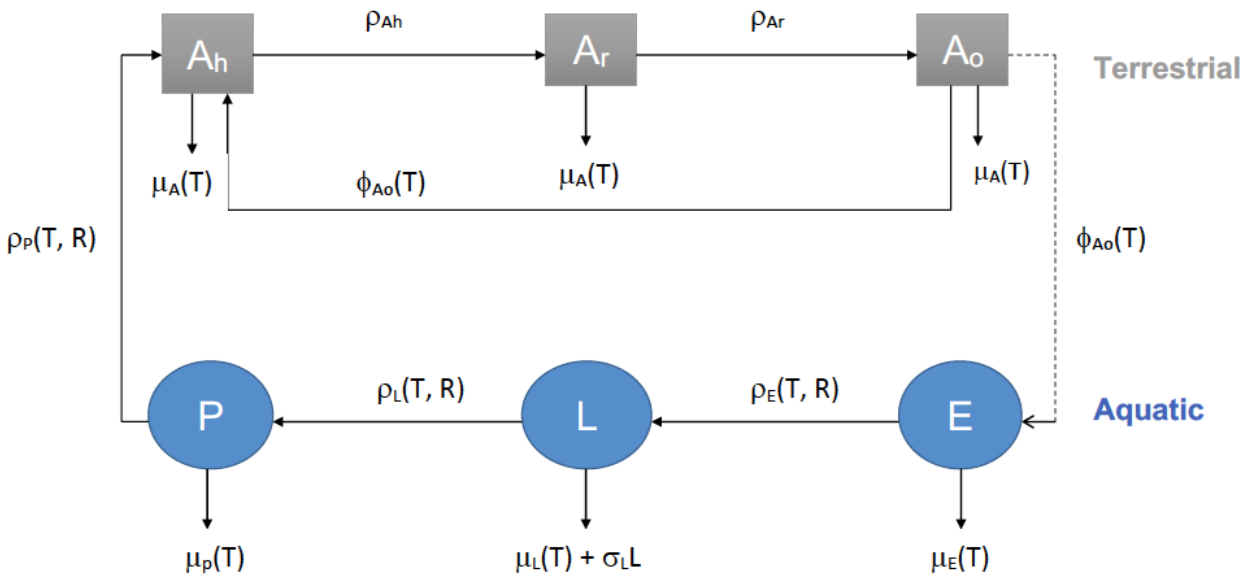

Figure 1: Flow diagram illustrating the model setup (see Equation 2.1), depicting the influence of temperature and rainfall on life history parameters. Density-dependent mortality (δ_L) occurs exclusively during the larval stage.

Table 1: Description of variables and parameters of the model (see Equation (2.1)).

Variable/ Parameter	**Description**	**Unit**
$E(t)$	Total number of eggs at time t	number
$L(t)$	Total number of larvae at time t	number
$P(t)$	Total number of pupae at time t	number
$A_h(t)$	Total number of host-seeking adult female mosquitoes at time t	number
$A_r(t)$	Total number of adult female mosquitoes at rest for egg development at time t	number
$A_o(t)$	Total number of adult female mosquitoes seeking oviposition site at time t	number
b	Total number of eggs laid per oviposition	number
$\phi_{Ao}(T)$	Eggs oviposition rate	time^{-1}
$\rho_E(T,R)$	Eggs hatching/development rate	time^{-1}
$\rho_L(T,R)$	Larvae development rate into pupae	time^{-1}
$\rho_P(T,R)$	Pupae development rate into female adult mosquitoes	time^{-1}
$\mu_E(T)$	Egg mortality rate	time^{-1}
$\mu_L(T)$	Larvae mortality rate	time^{-1}
$\mu_P(T)$	Pupae mortality rate	time^{-1}
$\mu_A(T)$	Adult mosquito mortality rate	time^{-1}
δ_L	Density-dependent mortality rate of Larvae	—
ρ_{Ah}	Rate at which host-seeking adult gets a blood meal and goes to rest	time^{-1}
ρ_{Ar}	Rate at which adult at rest enter into the oviposition searching state	time^{-1}
K	Environment carrying capacity of egg-laying female adult mosquitoes	—

2.2 Parameterization and data

The parameter estimates utilized in the model predominantly rely on data obtained from laboratory studies for *Anopheles* mosquito. To determine the functional relationships in the model, we employ nonlinear least squares optimization (NLS) and the method of maximum likelihood estimation (MLE).

For the parameterization of temperature-dependent mortality rates in the juvenile mosquito stages, we drew upon data from two studies conducted by Bayoh & Lindsay [38, 39], which were also used in [28]. These studies investigated mortality at varying constant temperatures using *An. gambiae* mosquitoes, the primary African malaria vector (refer to Appendix A.2). The data indicates a Gaussian dependence of mortality, as expressed by equations 2.4.

$$\mu_i(T) = \alpha_i \exp\left(\left(\frac{T(t) - T_i}{\gamma_i}\right)^2\right), \tag{2.4}$$

where $i = (E, L, P)$.

Additionally, the data for temperature-dependent mortality rates in the adult stage originated from a laboratory study to investigate the development and survival of *An. gambiae* at various temperatures [41]. The function that best fits the adult mortality data is shown in equation 2.5. This functional form 2.5 was also used in [28] to model adult mortality.

$$\mu_A(T) = \alpha_A \exp\left(\left(\frac{T(t) - T_A}{\gamma_A}\right)^4\right) \tag{2.5}$$

To parameterize the temperature-dependent adult gonotrophic cycle rate, we utilized data obtained from a research study conducted on *An. pseudopunctipennis* at various constant temperatures [42] (refer to Figure A.2). The data can be accurately represented by

$$\phi_{Ao}(T) = \alpha_G \exp\left(-\frac{(T(t) - T_G)^2}{\gamma_G}\right). \tag{2.6}$$

Moreover, to parameterize temperature- and rainfall-dependent developmental rates, we referred to laboratory studies on *Anopheles gambiae* and *Anopheles arabiensis*, as compiled by Depinay et al. [43] and Parham et al, [44]. The data from [44] for the average development times of immature stages τ_i suggest that the functional relation takes the form

$$\tau_i(T) = a + b\left(1 + \left(\frac{T(t)}{c}\right)^d\right)^{-1}, \quad i = \{E, L, P\}. \tag{2.7}$$

The expression for τ_i follows that which was used in [44] but with slightly different parameter values which were obtained by fitting the function to data to estimate the parameters, a, b, c, and d.

The maturation rate of eggs into larvae and pupae (into female adult mosquitoes) are defined using the function used in the supplemental material in [44] given by

$$\rho_i(T, R) = \frac{p_i(T, R)}{\tau_i(T)}, \quad i = \{E, L, P\}, \tag{2.8}$$

where $\tau_i(T) > 0$ is the average duration of each Stage i, given by 2.7 and $p_i(T, R)$, (where $0 \geq p_i(T, R) < 1$) is the daily survival probability of immature mosquitoes in Stage i (assumed

to be dependent on the mean daily temperature (T°C) and cumulative daily rainfall (R mm), so that

$$p_i(T, R) = p_i(T)p_i(R) \tag{2.9}$$

It is worth noting that there may be interactions between temperature and rainfall [28, 45]; however, the nature of the relationship is not clearly studied and therefore we are not integrating that into the model. Hence, we assume independent effects of temperature and rainfall on the daily survival probability of immature mosquitoes (consistent with the assumptions made in [46, 44, 12]). We also assume that development time at each stage is dependent only on temperature if there is adequate rainfall to sustain development [44]. Following [44, 46], the daily survival probability of immature mosquitoes in Stage i due to temperature is given by

$$p_i(T) = \exp(-\mu_i(T)) \tag{2.10}$$

Also, following the study in the supplementary material of [44] and the work done in [46], the rainfall-dependent daily survival probability of immature mosquitoes, $p_i(R)$ is given by

$$p_i(R) = R(R_{IM} - R)\left(\frac{4P_{Mi}}{R_{IM}^2}\right), \quad i = \{E, L, P\}, \tag{2.11}$$

where P_{Mi} is the peak daily survival probability of immature mosquito in stage i and $R_{IM} > R(t) > 0$, for all t, is the rainfall threshold peculiar to the region beyond which wash out effects from excessive rainfall cause no immature mosquitoes to survive.

The aforementioned parameter functions given by equations 2.4, 2.5 and 2.6 are plotted in figure 10 in the Appendix. For the development rate functions 2.8, we use mean monthly temperature and rainfall data from Ain Mahbel, Algeria to produce the figures (see the appendix 3 for details about the data). Numerical simulations of the model are carried out using temperature and rainfall profiles of four cities in East, West, North, and South Africa (see figure 2). These regions exhibit diverse seasonality patterns, ranging from year-round mosquito presence in Kumasi, Ghana, and Nairobi, Kenya, to a markedly seasonal mosquito abundance in Ain Mahbel, Algeria, and Cape Town, South Africa [47]. The primary mosquito species utilized for gathering data to estimate parameters are *Anopheles* mosquitoes; however, this model can be used as a robust to encompass the study of various other mosquito species.

2.3 Numerical Analysis

The numerical solutions of the model 2.1 are obtained using the deSolve package in R. This investigation aims to explore the impact of local environmental conditions, specifically temperature, and rainfall, on mosquito population dynamics and stage structure. The parameterized functions detailed in Section 2.2 and the constant parameters outlined in Table 2 are employed for the analysis of the model.

3 Results

In our analysis of the four considered regions in Africa, it became evident that neglecting seasonality leads to significant overestimation or underestimation of mosquito abundance.

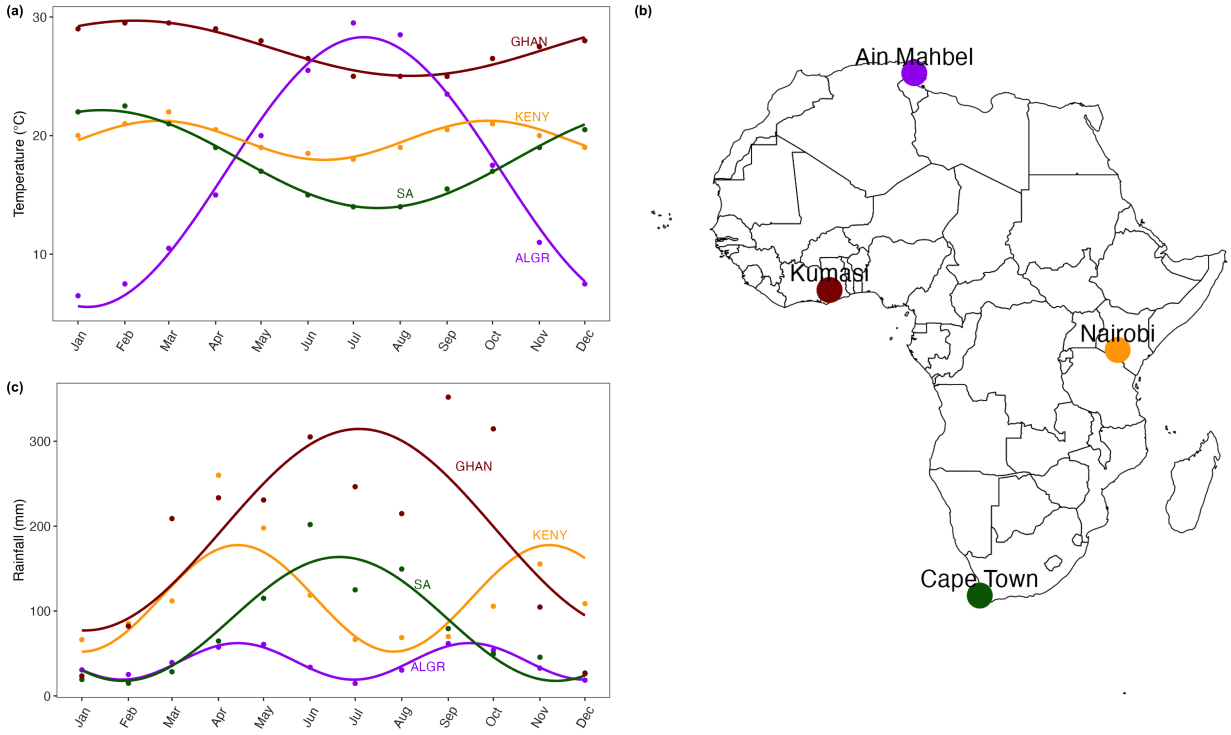

Figure 2: Weather data for the four African regions and their corresponding locations. (a) and (c) depict the average ambient temperature and rainfall patterns over twelve years. (b) A map of Africa illustrates the diverse locations where data was collected to inform the model 2.1.

Figure 3 illustrates the comparison between constant and seasonal environmental conditions. For Ain Mahbel, Algeria, disregarding seasonality results in an underestimated mosquito population. However, when seasonality is taken into account, we observe a substantial mosquito population, particularly during June to October. Conversely, in Ghana, neglecting seasonality leads to an overestimation of the total mosquito abundance for the year compared to when seasonality is considered. Specifically, in Algeria, the estimated annual mosquito abundance is approximately 11,434 when seasonality is ignored. This number is about ten times less than the population estimated when seasonality is considered.

We find that in different regions mosquitoes have different population dynamics (Figure 4). The region with warmer temperatures and higher rainfall (Kumasi, Ghana) across the year seems to have higher mosquito abundance (Figure 4b). Conversely, the region with cold temperatures and moderate rainfall (Cape Town, South Africa) has a much smaller mosquito abundance and peaks once for the entire year with mosquito numbers averaging around 11,426 which is about 25 times less than the estimated value in Ghana. The cold weather give rise to declines in the number of larvae that emerge as adults but these abundances rebound when environmental conditions become favourable as seen in Figures (4c-f). The smaller population size during the months of November-May in Algeria and June-January in South Africa is most likely due to the cold temperatures (Figure 4c-f) resulting in longer juvenile development times leading to a small number of larvae emerging as adults. Figure (4c-f) shows that temperature and rainfall may greatly impact mosquito stage structure.

Figure 5 reveals that mosquito abundance may vary across different months between regions. The region with warmer temperatures and higher rainfall (Kumasi, Ghana) estimates two peaks (that is in May and November) when temperature and rainfall values are in the range [26-28]°C and [104-230]mm respectively. The region with colder temperatures, Algeria, exhibits one peak during September when temperature and rainfall values are 23.5°C and 62mm. In Kenya, characterized by relatively mild and stable environmental conditions with less pronounced seasonality (see Figure 2), we observe a substantial presence of vectors throughout the year, with a significant fraction observed each month. Each of the regions peaks at different months and different levels. This implies that the timing of mosquito control implementation may differ for different regions.

To assess the optimal timing and duration of mosquito control interventions throughout the year, we calculated the cumulative fraction of mosquitoes for each region (see Figure 6a). Our findings reveal that in regions with colder temperatures, such as Algeria and South Africa, approximately 50% of the annual mosquito population can be controlled by focusing interventions on just two months. For instance, in Algeria, targeting control measures during August and September could prevent half of the mosquito population for the entire year. Conversely, in warmer regions, such as Kenya, vector control efforts may need to be intensified over a longer period, spanning approximately 4 to 5 months, to achieve a similar level of control. Our analysis suggests that in Kenya, implementing controls from December to May could cover 50% of the annual mosquito abundance. Furthermore, our results indicate variations in the optimal timing of control strategies between regions, as illustrated in Figure 6b. Specifically, regions like Ghana and Kenya may require continuous vector control efforts throughout the year, whereas in Algeria and South Africa, vector controls may be concentrated within a few months.

Figures 7 and 8 illustrate the correlation between mosquito abundance and human deaths attributed to malaria across the various regions from 2015 to 2019. Mosquito abundance data, generated from model 2.1, is compared with malaria-related mortality data obtained from

the Institute for Health Metrics and Evaluation (IHME), Global Burden of Disease (2019) [48]. Notably, regions with higher mosquito abundance, such as Ghana, consistently exhibit elevated levels of malaria-related deaths during the study period (see Figure 8). Conversely, regions with lower mosquito populations correspondingly report fewer malaria deaths. This underscores a strong correlation between mosquito abundance and total human mortality. However, Algeria presents a distinct pattern; despite estimating a significant mosquito population, no malaria-related deaths are reported during this period. This anomaly can be attributed to Algeria's official recognition by the World Health Organization (WHO) as malaria-free, making it the second country in the WHO African region to achieve this status. Algeria recorded its last indigenous malaria cases in 2013 [49] which is before the period considered in this study. In Figure 7, we observe that there is no consistent pattern regarding the relationship between the number of malaria deaths and mosquito abundance across the various regions over the five years. While the mosquito population appears relatively stable with only minor fluctuations from year to year, the number of malaria deaths displays variability across different years (2015-2019). For instance, in South Africa, despite estimating the highest mosquito population, the lowest number of malaria deaths was recorded in 2015. Similarly, in Kenya, there is a notable increase in malaria deaths from 2015 to 2019, despite minor fluctuations in mosquito abundance during this period. This discrepancy could potentially be attributed to the implementation of varying mosquito control measures at different times throughout the year.

To assess performance, the model 2.1 is compared with *Anopheles* species abundance data collected from different sites within the regions of consideration. Certainly, the environments for the various regions for which mosquitoes were collected are not free from vector control, which may affect the number of mosquitoes collected. Further details on mosquito collection and experimental procedures can be found in [cite here ie. put the papers where the data are taken from over here]. In Figure 8, we show the comparison of estimated mosquito abundance to actual mosquito counts for the different regions. We find that in one site in South Africa, there is a close correlation between the model estimates and the actual mosquito count data (Figure 6a) (the model produces a similar curve with the mosquito count data) except that the peak times differ. For Ghana, the model agrees with the data at some points and it deviates at some other points as shown in Figure 6c. For Kenya, the data for the different sites do not correlate with the model's estimates. This may be due to poor collection at the collection centers and the fact that the collection sites have vector control implemented reducing the number of vectors available to be trapped and counted.

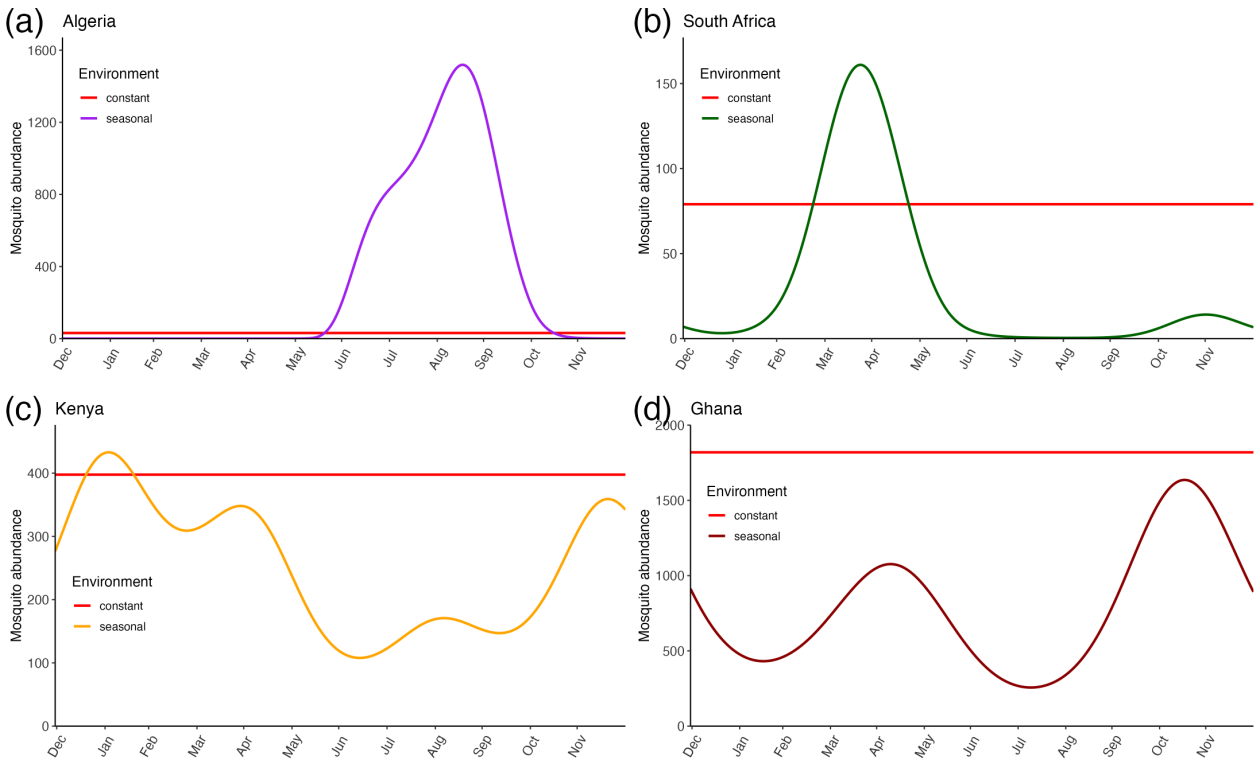

Figure 3: Numerical simulation of the model 2.1 illustrating the abundance of female adult mosquitoes in four African cities, comparing the population dynamics under constant and seasonal environmental conditions. **(a)** Ain Mahbel, Algeria ($R_{IM} = 60$mm), **(b)** Kumasi, Ghana ($R_{IM} = 550$mm), **(c)** Nairobi, Kenya ($R_{IM} = 200$mm), and **(d)** Cape Town, South Africa ($R_{IM} = 250$mm).

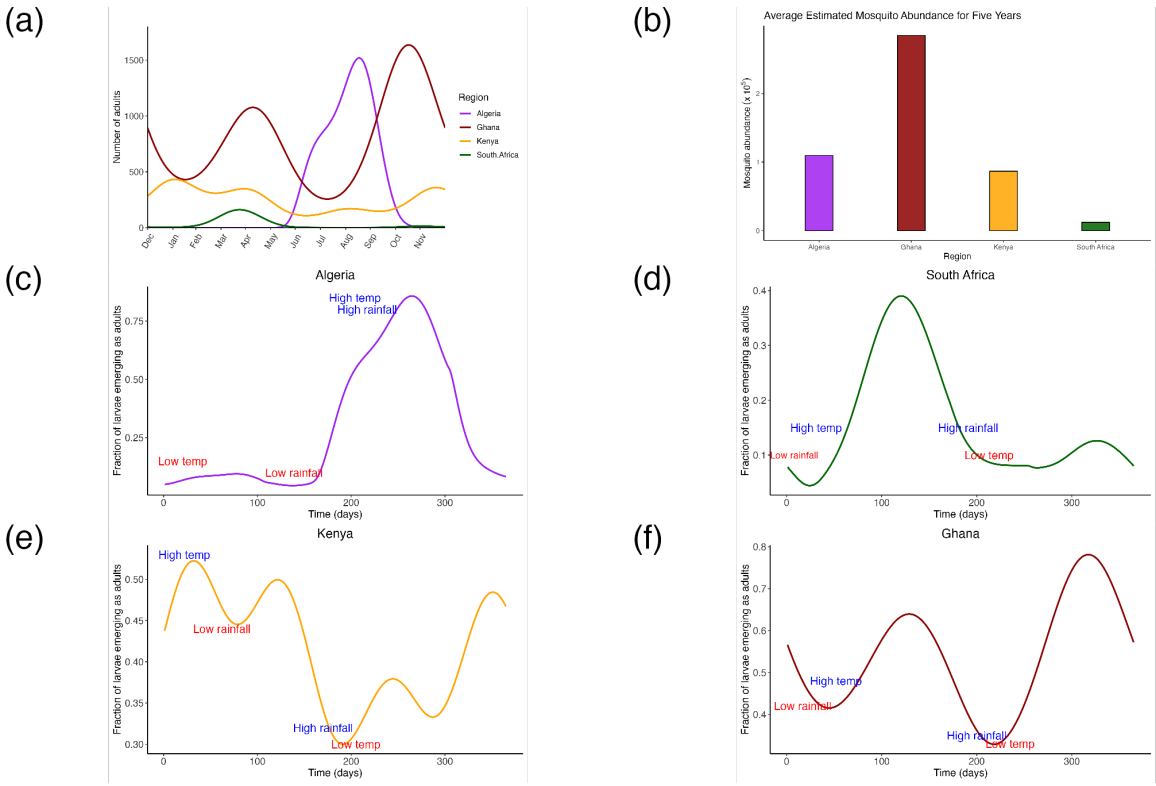

Figure 4: Numerical solution of the stage-structured model. All figures present results from the 5th-year simulation to mitigate initial condition effects. (a) Monthly dynamics of adult female mosquito populations compared across four African cities. (b) Yearly total abundance estimates for each region. (c) Daily fraction of larvae emerging as adult mosquitoes in Algeria. (d) Daily fraction of larvae emerging as adult mosquitoes in South Africa. (e) Daily fraction of larvae emerging as adult mosquitoes in Kenya. (f) Daily fraction of larvae emerging as adult mosquitoes in Ghana.

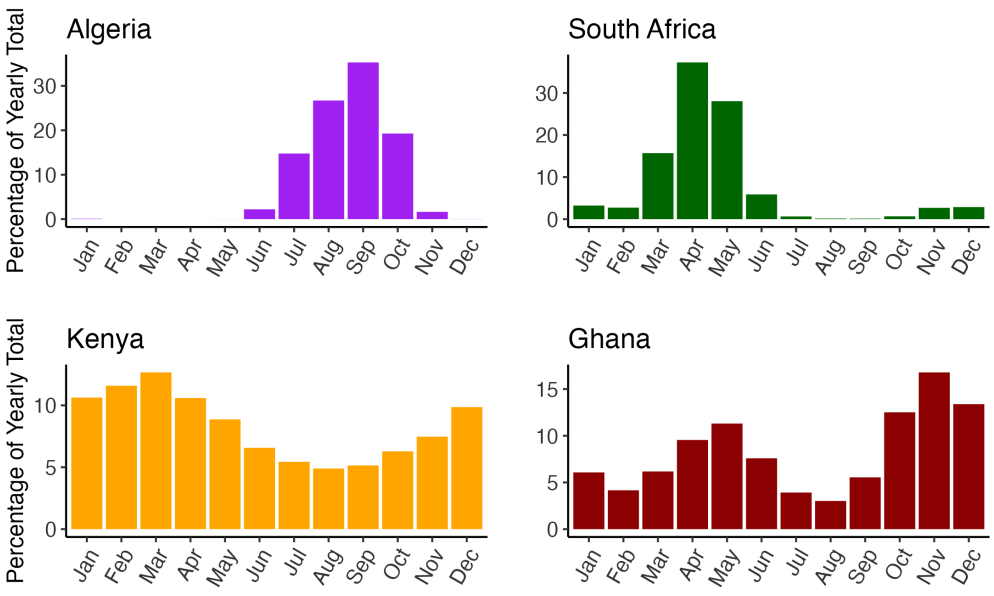

Figure 5: Model simulations illustrating the monthly distribution of adult female mosquitoes as a percentage of the yearly total across regions. Results are averaged over a five-year simulation period.

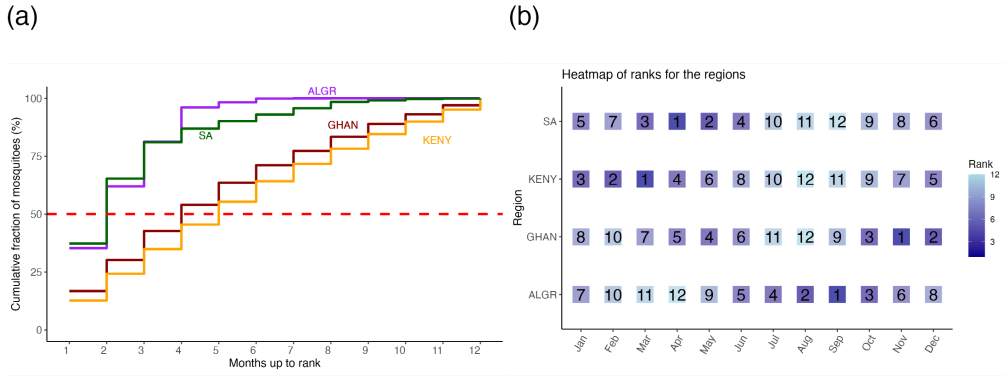

Figure 6: Examining the optimal timing for mosquito control strategies, we calculated the cumulative fraction of mosquitoes for each region. This analysis highlights specific months requiring concentrated control efforts to effectively reduce mosquito populations. Notably, in Algeria and South Africa, over half of the mosquito population is concentrated within two months. Focusing control measures during these months could significantly diminish mosquito populations and consequently mitigate the spread of diseases.

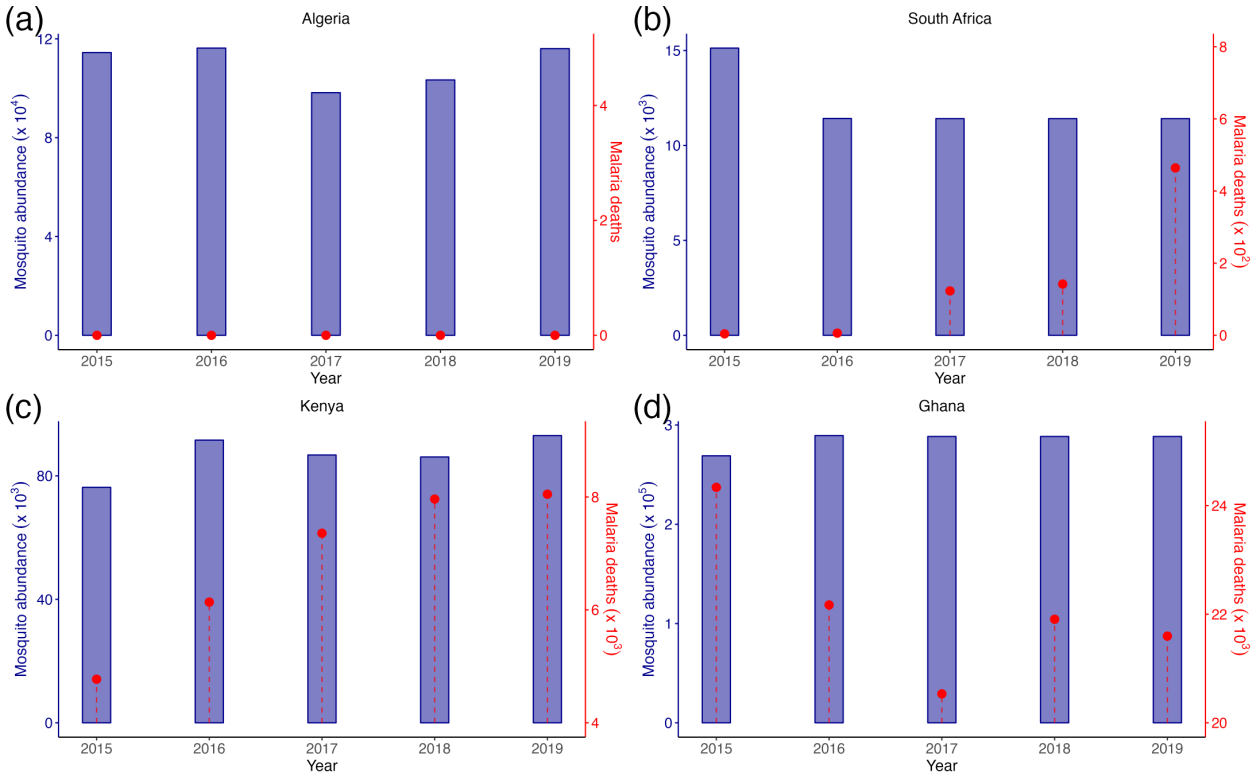

Figure 7: Model simulations (2.1) illustrating the estimated total abundance of adult female *Anopheles* mosquitoes, overlaid with human malaria-related death data for the four regions from 2015 to 2019. Malaria death data sourced from IHME, Global Burden of Disease (2019).

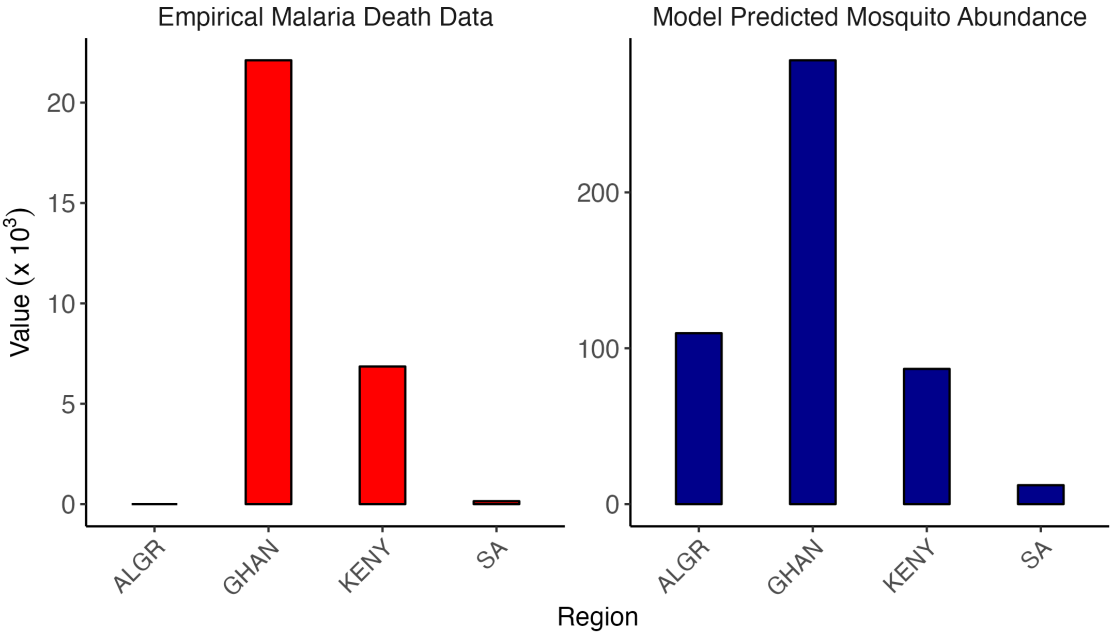

Figure 8: Comparison of malaria deaths and mosquito abundance by region.

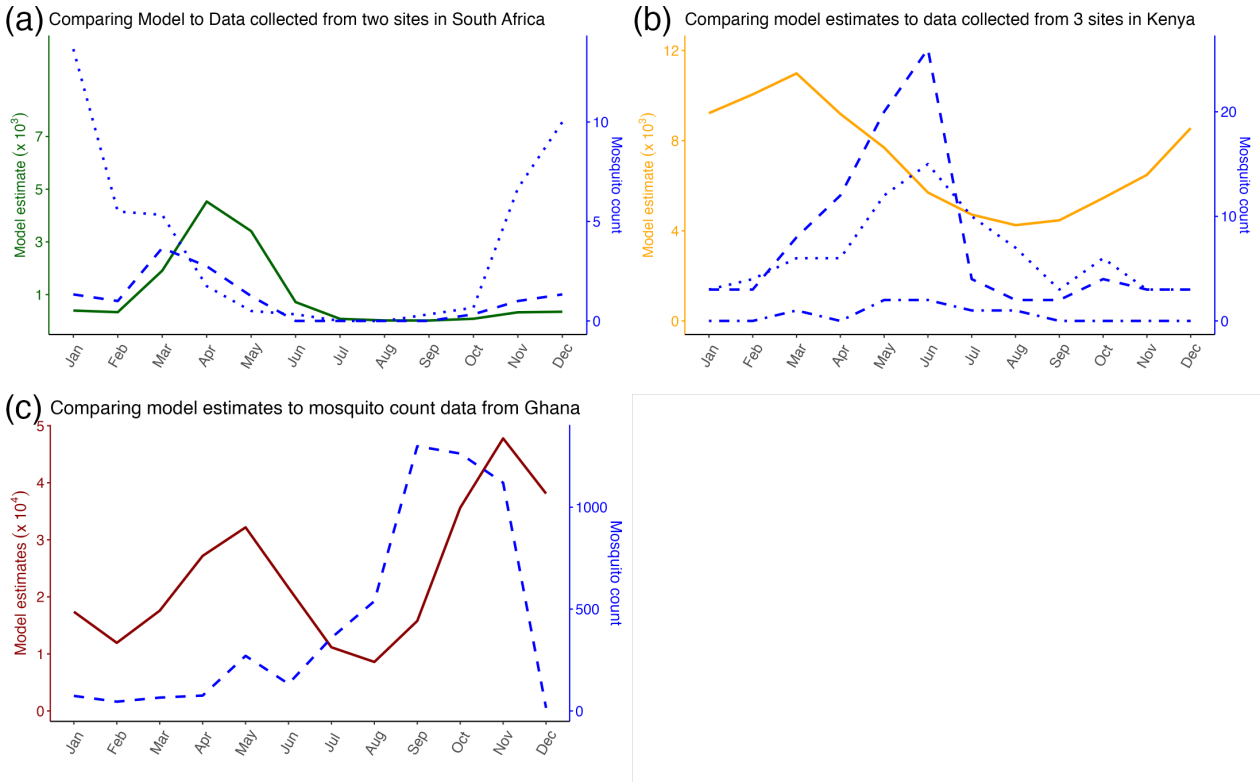

Figure 9: Comparing average *Anopheles* mosquito count data with simulated monthly mosquito abundance for (a) South Africa, (b) Kenya, and (c) Ghana.

4 Discussion

Our findings underscore the importance of considering regional seasonality in weather for accurate modelling of mosquito population dynamics and stage structure. Understanding these dynamics is crucial for effective vector-borne disease outbreak prediction and vector management strategies in different regions. The analysis reveals that incorporating seasonality in environmental conditions is essential, as neglecting it may lead to biased predictions, as evidenced in Figure 3. Therefore, integrating seasonality into models that estimate vector population dynamics is imperative for more reliable predictions and informed decision-making in vector control efforts.

The dynamics of mosquitoes in regions with colder temperatures, such as Algeria and South Africa, exhibit similarities, characterized by large peaks during favourable environmental conditions with reduced populations during other periods (Figure 4a). Conversely, in relatively warmer regions like Ghana, mosquitoes persist throughout the year, with consistently high population estimates. Kenya experiences a moderate range of temperatures and varied rainfall, leading to mosquito persistence at lower levels compared to Ghana. Regions with colder temperatures, such as Algeria and South Africa, experience population declines during colder months, followed by rebounds and population increases during warmer periods (Figure 4a, c, d).

Our analysis reveals distinct patterns in mosquito abundance across different months and regions, as depicted in Figure 5. Regions experiencing warmer temperatures and higher rainfall, like Kumasi, Ghana, exhibit two peaks in mosquito abundance in May and November, coinciding with optimal environmental conditions for mosquito development. During these months, reduced development times lead to accelerated juvenile maturation to the adult stage. Conversely, colder regions such as Algeria show a single peak in September. Interestingly, regions like Kenya, with milder and less seasonal environmental conditions, maintain a consistent presence of mosquito vectors throughout the year. These findings suggest the importance of tailoring mosquito control efforts to specific environmental conditions. In colder regions like Algeria and South Africa, focusing vector management efforts during peak periods could significantly reduce mosquito populations and control disease spread. However, the effectiveness of control measures may vary due to regional environmental variations. Therefore, adaptive and context-specific vector control strategies are essential to reduce mosquito populations and mitigate mosquito-borne diseases effectively.

Our analysis reveals varying durations of control implementation across regions, reflecting differences in local environmental conditions. Regions with warmer temperatures and higher rainfall exhibit higher mosquito populations year-round, necessitating continuous vector control efforts. Conversely, regions with colder temperatures experience minimal mosquito populations during certain periods, requiring control measures only during select months. This insight underscores the importance of identifying critical periods for mosquito control to effectively reduce populations and mitigate disease spread.

The analysis of malaria mortality data underscores a significant correlation between mosquito abundance and malaria deaths during the period from 2015 to 2019 (see Figure 8). Ghana, estimating the highest mosquito populations throughout the year among the regions studied, also reports the highest malaria deaths. Conversely, Algeria, despite estimating a substantial mosquito population, reports zero malaria deaths during the same period. This anomaly is attributed to Algeria's achievement of malaria-free status, certified by the World Health Organization (WHO) during this time [49]. Algeria's success in combating

the disease can be attributed to various factors, including a well-trained health workforce, universal healthcare providing malaria diagnosis and treatment, prompt responses to disease outbreaks, and vector control efforts. Algeria's example provides valuable lessons for other regions in Africa, demonstrating that malaria elimination is attainable through concerted efforts, strategic investments, and evidence-based approaches.

Upon superimposing estimates derived from the model with actual mosquito collection data (Figure 7), a notable lack of agreement between the two sets of data becomes apparent. This discrepancy may stem from biases inherent in the methods used for mosquito collection at various collection centers. To address this issue, we advocate for intensified research efforts aimed at refining mosquito collection techniques. By improving the accuracy and reliability of mosquito collection methods, researchers can ensure the availability of high-quality data for validating and refining mathematical models used in mosquito population dynamics studies. This, in turn, will enhance the robustness and applicability of such models, facilitating more accurate predictions and informed decision-making in vector control strategies and disease management efforts.

It's important to highlight that our model formulation does not explicitly account for adult males. Instead, it assumes that their abundance is equal to that of adult females. This simplification is rooted in the epidemiological significance of female mosquitoes. Unlike their male counterparts, female mosquitoes serve as vectors responsible for transmitting pathogens because they require a blood meal for egg production. While males play a role in reproduction, they do not contribute to disease transmission as they do not feed on blood. Therefore, for epidemiological relevance, assuming equal abundance between adult males and females is justified. This simplification helps streamline the model's complexity without compromising its accuracy in investigating mosquito dynamics.

While our model provides valuable insights into mosquito population dynamics and their response to environmental conditions, several limitations should be noted. Firstly, the model simplifies certain biological processes by not explicitly considering adult male mosquitoes in the formulation. While we assume equal abundance between adult males and females, this simplification may overlook potential differences in behaviour and ecology between the sexes that could influence population dynamics. Additionally, our model primarily focuses on the *Anopheles* species, a significant malaria vector, potentially neglecting the dynamics of other mosquito species present in the study regions, such as the *Aedes* mosquito in South Africa, and their interactions with *Anopheles*. It is important to note that the potential presence of other mosquito species leading to intra-specific competitions may impact local dynamics (as discussed in [11]). Furthermore, the model assumes homogeneity in environmental conditions within each region, disregarding potential micro-climatic variations that could impact mosquito population dynamics. Moreover, while temperature and rainfall data are incorporated into the model, other important factors like habitat suitability, land use changes, and human interventions (e.g., vector control measures) are not explicitly considered, despite their potential impact on mosquito populations. The accuracy of our model estimates is also dependent on the quality of input data, including parameter estimates and environmental variables, which may vary in availability and reliability across regions. Additionally, the use of monthly averaged temperature and rainfall data may not adequately capture micro-fluctuations in environmental conditions, as daily data were not readily available for most study regions. Furthermore, the model fitting to temperature and rainfall data was not optimal in some regions (see figure 2 and table 3), potentially affecting the accuracy of the model estimates. Therefore, while our model offers valuable insights, further refinements and

validations are necessary to improve its robustness and applicability.

Our study investigates the influence of local temperature and rainfall conditions on mosquito population dynamics across diverse regions. To facilitate a thorough comparison, we ensure consistency in all other factors and parameters across the study areas. Our model is specifically designed to capture the intricate behaviour of the *Anopheles* species, a key vector responsible for malaria transmission and prevalent in the regions under consideration. Through our model analysis, we obtain profound insights into the intricate interplay between environmental factors and mosquito population dynamics, thereby enriching our understanding of optimal timing for vector control implementation and vector-borne disease transmission dynamics.

5 Conclusion

This study formulates a temperature- and rainfall-dependent stage-structured model, shedding light on the influence of regional weather variability on mosquito population dynamics and stage structure across Ain Mahbel, Algeria, Cape Town, South Africa, Nairobi, Kenya, and Kumasi, Ghana. The observed variations in mosquito population dynamics among these regions emphasize the necessity of accounting for local weather conditions in vector control planning. The identification of peak mosquito months provides invaluable insights for the formulation of targeted intervention strategies. Moreover, the correlation between mosquito dynamics and malaria-related deaths underscores the potential implications for disease outbreak risk and duration. These findings significantly contribute to our broader comprehension of vector-borne disease dynamics and provide a foundation for the development of region-specific vector control strategies aimed at mitigating outbreak risks.

Future research avenues may extend the scope of this study to include other regions where malaria is endemic. Additionally, there is a need to explore the integration of additional environmental factors such as humidity to obtain a more comprehensive understanding of the impact of environmental conditions on mosquito population dynamics and the risk of disease transmission.

Acknowledgements: Amy Hurford acknowledges financial support from the Natural Sciences and Engineering Research Council of Canada (NSERC) through Discovery Grant RGPIN-2023-05905. The authors gratefully acknowledge the valuable feedback provided by members of the Hurford lab.

Statements and Declarations

Amy Hurford acknowledges financial support from the Natural Sciences and Engineering Research Council of Canada (NSERC) through Discovery Grant RGPIN RGPIN-2023-05905.

References

[1] World Health Organization. *Malaria*. 2023. URL: https://www.who.int/news-room/questions-and-answers/item/malaria?gclid=Cj0KCQjwiIOmBhDjARIsAP6YhSWppktVtmrCQQTmq7L3f97SZPuwUMwNfJ6k4Ij-2NIGq4qKo3udUVIaAl_7EALw_wcB (visited on 07/26/2023).

[2] Arielle Witter. 6 Facts You Didn't Know About Malaria. https://www.one.org/international/blog/facts-about-malaria/?gad=1&gclid=Cj0KCQjwiIOmBhDjARIsAP6YhSXYnDNoVF5bMwSA5MdcrrpRg57OLZgmbFvZU2Au61XsqlKJ1dPoHOMaAqJ5EALw_wcB. Accessed: 2023-07-26. 2023.

[3] Erin A Mordecai et al. Climate change could shift disease burden from malaria to arboviruses in Africa. In: *The Lancet Planetary Health* 4.9 (2020), e416–e423.

[4] Bayissa Chala and Feyissa Hamde. Emerging and re-emerging vector-borne infectious diseases and the challenges for control: A review. In: *Frontiers in public health* 9 (2021), p. 715759.

[5] S Manikandan et al. A review on vector borne disease transmission: Current strategies of mosquito vector control. In: *Indian Journal of Entomology* (2023), pp. 503–513.

[6] Antonio Ligsay, Olivier Telle, and Richard Paul. Challenges to mitigating the urban health burden of mosquito-borne diseases in the face of climate change. In: *International Journal of Environmental Research and Public Health* 18.9 (2021), p. 5035.

[7] Elizabeth Ivanovich. 5 REASONS TO JOIN THE FIGHT AGAINST MALARIA. https://unfoundation.org/blog/post/5-reasons-to-join-the-fight-against-malaria/?gclid=Cj0KCQjwiIOmBhDjARIsAP6YhSUdLH6qSDz1rQF3RTiTBxtW-LW0oaz6m5dlqgGF5QV8_-l-5KcNJFwaAqhREALw_wcB. Accessed: 2023-07-27. 2014.

[8] World Health Organization et al. *A global brief on vector-borne diseases*. Tech. rep. World Health Organization, 2014.

[9] World Health Organization. *Global Malaria Programme*. 2024. URL: https://www.who.int/teams/global-malaria-programme/elimination/countries-and-territories-certified-malaria-free-by-who (visited on 03/21/2024).

[10] Chris Robbins et al. Assessing topical treatment interventions on Scottish salmon farms using a sea lice (Lepeophtheirus salmonis) population model. In: *Aquaculture* 306.1-4 (2010), pp. 191–197.

[11] Amy Hurford, Xiunan Wang, and Xiao-Qiang Zhao. Regional climate affects salmon lice dynamics, stage structure and management. In: *Proceedings of the Royal Society B* 286.1904 (2019), p. 20190428.

[12] Ahmed Abdelrazec and Abba B Gumel. Mathematical assessment of the role of temperature and rainfall on mosquito population dynamics. In: *Journal of mathematical biology* 74.6 (2017), pp. 1351–1395.

[13] Priscilla Cailly et al. A climate-driven abundance model to assess mosquito control strategies. In: *Ecological Modelling* 227 (2012), pp. 7–17.

[14] EA Mordecai et al. A, Pawar S, Ryan SJ, Smith TC, Lafferty KD. 2013. In: *Optimal temperature for malaria transmission is dramatically lower than previously predicted. Ecology Letters* 16.1 (), pp. 22–30.

[15] Jeffrey Shaman and Jonathan F Day. Reproductive phase locking of mosquito populations in response to rainfall frequency. In: *PLoS one* 2.3 (2007), e331.

[16] Pei-Chih Wu et al. Higher temperature and urbanization affect the spatial patterns of dengue fever transmission in subtropical Taiwan. In: *Science of the total Environment* 407.7 (2009), pp. 2224–2233.

[17] Nur'Izzati Hamdan and Adem Kilicman. The effect of temperature on mosquito population dynamics of Aedes aegypti: The primary vector of dengue. In: *AIP Conference Proceedings*. Vol. 2266. 1. AIP Publishing. 2020.

[18] David Andrew Ewing et al. Modelling the effect of temperature on the seasonal population dynamics of temperate mosquitoes. In: *Journal of theoretical biology* 400 (2016), pp. 65–79.

[19] Jiafeng Wang, Nick H Ogden, and Huaiping Zhu. The impact of weather conditions on Culex pipiens and Culex restuans (Diptera: Culicidae) abundance: a case study in Peel region. In: *Journal of medical entomology* 48.2 (2011), pp. 468–475.

[20] HMl Yang et al. Assessing the effects of temperature on the population of Aedes aegypti, the vector of dengue. In: *Epidemiology & Infection* 137.8 (2009), pp. 1188–1202.

[21] Gbenga J Abiodun et al. Modelling the influence of temperature and rainfall on the population dynamics of Anopheles arabiensis. In: *Malaria journal* 15.1 (2016), pp. 1–15.

[22] Christopher Mitchell and Christopher Kribs. A comparison of methods for calculating the basic reproductive number for periodic epidemic systems. In: *Bulletin of mathematical biology* 79.8 (2017), pp. 1846–1869.

[23] FB Agusto, AB Gumel, and PE Parham. Qualitative assessment of the role of temperature variations on malaria transmission dynamics. In: *Journal of Biological Systems* 23.04 (2015), p. 1550030.

[24] Hau V Pham et al. Ecological factors associated with dengue fever in a Central Highlands province, Vietnam. In: *BMC infectious diseases* 11.1 (2011), pp. 1–6.

[25] Hyun Mo Yang et al. Follow up estimation of Aedes aegypti entomological parameters and mathematical modellings. In: *Biosystems* 103.3 (2011), pp. 360–371.

[26] Angelina Mageni Lutambi et al. Mathematical modelling of mosquito dispersal in a heterogeneous environment. In: *Mathematical biosciences* 241.2 (2013), pp. 198–216.

[27] Kamaldeen Okuneye and Abba B Gumel. Analysis of a temperature-and rainfall-dependent model for malaria transmission dynamics. In: *Mathematical biosciences* 287 (2017), pp. 72–92.

[28] Lindsay M Beck-Johnson et al. The effect of temperature on Anopheles mosquito population dynamics and the potential for malaria transmission. In: *PLOS one* 8.11 (2013), e79276.

[29] Xiunan Wang and Xingfu Zou. Threshold dynamics of a temperature-dependent stage-structured mosquito population model with nested delays. In: *Bulletin of mathematical biology* 80 (2018), pp. 1962–1987.

[30] Teresa K Yamana and Elfatih AB Eltahir. Incorporating the effects of humidity in a mechanistic model of Anopheles gambiae mosquito population dynamics in the Sahel region of Africa. In: *Parasites & vectors* 6.1 (2013), pp. 1–10.

[31] Olugbenga O Oluwagbemi et al. ANOSPEX: a stochastic, spatially explicit model for studying Anopheles metapopulation dynamics. In: *PloS one* 8.7 (2013), e68040.

[32] Kamaldeen Okuneye, Ahmed Abdelrazec, and Abba B Gumel. Mathematical analysis of a weather-driven model for the population ecology of mosquitoes. In: *Mathematical Biosciences & Engineering* 15.1 (2018), pp. 57–93.

[33] EPA. *Mosquito Life Cycle*. 2023. URL: https://www.epa.gov/mosquitocontrol/mosquito-life-cycle#:~:text=All%20mosquito%20species%20go%20through,just%20before%20emerging%20as%20adult. (visited on 08/15/2023).

[34] CDC. *Mosquito life cycle*. 2023. URL: https://www.cdc.gov/dengue/resources/factsheets/mosquitolifecyclefinal.pdf (visited on 08/15/2023).

[35] Mosquito World - Your guide to effective home mosquito control. *The Mosquito Life Cycle: Four Distinct Stages*. 2023. URL: http://www.mosquitoworld.net/about-mosquitoes/life-cycle/ (visited on 08/15/2023).

[36] Mario Ignacio Simoy, Maria Veronica Simoy, and Graciela Ana Canziani. The effect of temperature on the population dynamics of Aedes aegypti. In: *Ecological modelling* 314 (2015), pp. 100–110.

[37] Samuel Rickard Christophers. *Aedes aegypti: the yellow fever mosquito*. CUP Archive, 1960.

[38] Mohamed N Bayoh and Steve W Lindsay. Effect of temperature on the development of the aquatic stages of Anopheles gambiae sensu stricto (Diptera: Culicidae). In: *Bulletin of entomological research* 93.5 (2003), pp. 375–381.

[39] Mohamed N Bayoh and Steve W Lindsay. Temperature-related duration of aquatic stages of the Afrotropical malaria vector mosquito Anopheles gambiae in the laboratory. In: *Medical and veterinary entomology* 18.2 (2004), pp. 174–179.

[40] Paul Edward Parham and Edwin Michael. Modeling the effects of weather and climate change on malaria transmission. In: *Environmental health perspectives* 118.5 (2010), pp. 620–626.

[41] Mohamed Nabie Bayoh. Studies on the development and survival of Anopheles gambiae sensu stricto at various temperatures and relative humidities. PhD thesis. Durham University, 2001.

[42] Frédéric J Lardeux et al. A physiological time analysis of the duration of the gonotrophic cycle of Anopheles pseudopunctipennis and its implications for malaria transmission in Bolivia. In: *Malaria journal* 7.1 (2008), pp. 1–17.

[43] Jean-Marc O Depinay et al. A simulation model of African Anopheles ecology and population dynamics for the analysis of malaria transmission. In: *Malaria journal* 3.1 (2004), pp. 1–21.

[44] Paul E Parham et al. Modeling the role of environmental variables on the population dynamics of the malaria vector Anopheles gambiae sensu stricto. In: *Malaria Journal* 11.1 (2012), pp. 1–13.

[45] Edith O Lyimo and JC Koella. Relationship between body size of adult Anopheles gambiae sl and infection with the malaria parasite Plasmodium falciparum. In: *Parasitology* 104.2 (1992), pp. 233–237.

[46] Godwin Ray Anugboba Okogun et al. Life-table analysis of Anopheles malaria vectors: generational mortality as tool in mosquito vector abundance and control studies. In: *Journal of vector borne diseases* 42.2 (2005), p. 45.

[47] Matthew E Cairns et al. Seasonality in malaria transmission: implications for case-management with long-acting artemisinin combination therapy in sub-Saharan Africa. In: *Malaria journal* 14 (2015), pp. 1–13.

[48] Max Roser and Hannah Ritchie. *Malaria*. 2024. URL: https://ourworldindata.org/malaria (visited on 03/14/2024).

[49] World Health Organization. *Algeria and Argentina certified malaria-free by WHO*. 2019. URL: https://www.who.int/news/item/22-05-2019-algeria-and-argentina-certified-malaria-free-by-who#:~:text=Algeria%20and%20Argentina%20reported%20their,in%202013%20and%202010%20respectively. (visited on 03/15/2024).

A Model description and parameterization

A.1 Model description

Here we derive the mathematical model describing mosquito dynamics (see equation 2.1). This model 2.1 is very similar to the models formulated in Abdelrazec & Gumel, (2017) [1] and also the model in Caily et. al., (2012) [2]. The major difference between our model and that of Abdelrazec & Gumel, (2017) [1] is that our model has the adult population subdivided into three stages $(A_h(t), A_r(t), A_o(t))$. Also comparing our model to Caily et. al., (2012), our model has the parameters depending on time.

Our mathematical model for mosquito population dynamics incorporates a temperature- and rainfall-dependent development rates and temperature-dependent mortality rates. We also incorporates density-dependent mortality in the laval stage. We note that temperature and rainfall are time-dependent.

Let $E(t), L(t), P(t)$ and $A(t)$ be the distinct life stages of the mosquito. Assuming that the adult females mate with the male counterparts just upon emerging from the pupa, we describe a stage-structured mathematical model as;

$$
\begin{aligned}
\frac{dE}{dt} &= b\phi_{A_0}(T)\left(1-\frac{A_o}{K}\right)A_0 - \left(\rho_E(T,R)+\mu_E(T)\right)E,\\
\frac{dL}{dt} &= \rho_E(T,R)E - \left(\rho_L(T,R)+\mu_L(T)+\sigma_L L\right)L,\\
\frac{dP}{dt} &= \rho_L(T,R)L - \left(\rho_P(T,R)+\mu_P(T)\right)P,\\
\frac{dA_h}{dt} &= \rho_P(T,R)P + \phi_{A_o}(T)A_o - \left(\rho_{A_h}+\mu_A(T)+\mu_{A_h}\right)A_h,\\
\frac{dA_r}{dt} &= \rho_{A_h}A_h - \left(\rho_{A_r}+\mu_A(T)\right)A_r,\\
\frac{dA_o}{dt} &= \rho_{A_r}A_r - \left(\phi_{A_o}(T)+\mu_A(T)+\mu_{A_o}\right)A_o,
\end{aligned}
\tag{A.1}
$$

The term $\phi_{A_0}(T)\,(1-A_o/K)$ represents the density-dependent eggs oviposition rate (where $K > A_o$) for all $t \geq 0$ is the environmental carrying capacity of female adult mosquitoes and $\phi_{A_0}(T)$ is the temperature-dependent egg deposition rate. Eggs hatch into larvae stage at a temperature- and rainfall-dependent rate, $\rho_E(T,R)$. Larvae mature into pupae at a temperature- and rainfall-dependent rate, $\rho_L(T,R)$. Pupae mature into the female adult mosquitoes at a temperature- and rainfall-dependent rate, $\rho_P(T,R)$. It should be stated that the development rates for the juvenile stages are dependent on temperature and rainfall because, while temperature values greatly impact developmental time of the juvenile mosquitoes [3, 4, 5, 6, 7, 8], rainfall is required for availability of breeding sites and habitats [8, 9, 10]. However, extreme environmental conditions such as too hot or too cold are not favourable for the survival and maturation of the larvae [11, 3, 4, 5, 6, 8] and also excessive rainfall washes out the larval breeding sites, such as small stagnant water on yards or lawn [1]. These newly emerged female adult mosquitoes mate with the males and quest for a blood meal. Upon successful feeding on a blood meal, they go to rest to allow for the eggs to develop at a rate ρ_{A_h}. The rested female with developed eggs seeks for oviposition site at a rate ρ_{A_r}. Ones the eggs are laid, it goes through the cycle again and the mosquito which laid the eggs also go into the adult seeking host stage to continue the cycle until it dies and leaves the cycle.

A.2 Data and parameter estimation

Description of all parameters are provided in table 1 in the main manuscript. Regional variations exist in temperature and rainfall, yet the functional relationships describing the model parameters with respect to temperature (T) and rainfall (R) remain consistent across diverse regions. The estimation of life history parameters as a function of temperature and/or rainfall involves curve fitting to laboratory experiment data utilizing functional forms based on previous studies [12, 13, 14, 15, 8, 10].

Our models' parameterization focuses on the *Anopheles* species of mosquitoes. These species are noted as the primary vector that transmit the malaria parasite in the African region. The data for temperature-dependent mortality rates in the adult stage originated from a laboratory study to investigate the development and survival of *An. gambiae* at various temperatures [13]. This study monitored mortality rates across a temperature range under various humidity conditions (refer to Figure A2). For our model, we specifically employed the adult mortality data recorded at 60% and 80% humidity, both of which are considered suitable humidity levels for *An. gambiae* mosquitoes [12]. The Gaussian function that best fits the adult mortality data resembles that of the juvenile stage but it is raised to power four instead of power two. This functional form was also used by Beck-Johnson et al, (2013) [12] to model adult mortality. The various functional forms used in describing the life history parameters are given in the main manuscript (see equations 2.4 - 2.11) with their figures shown in figure 10.

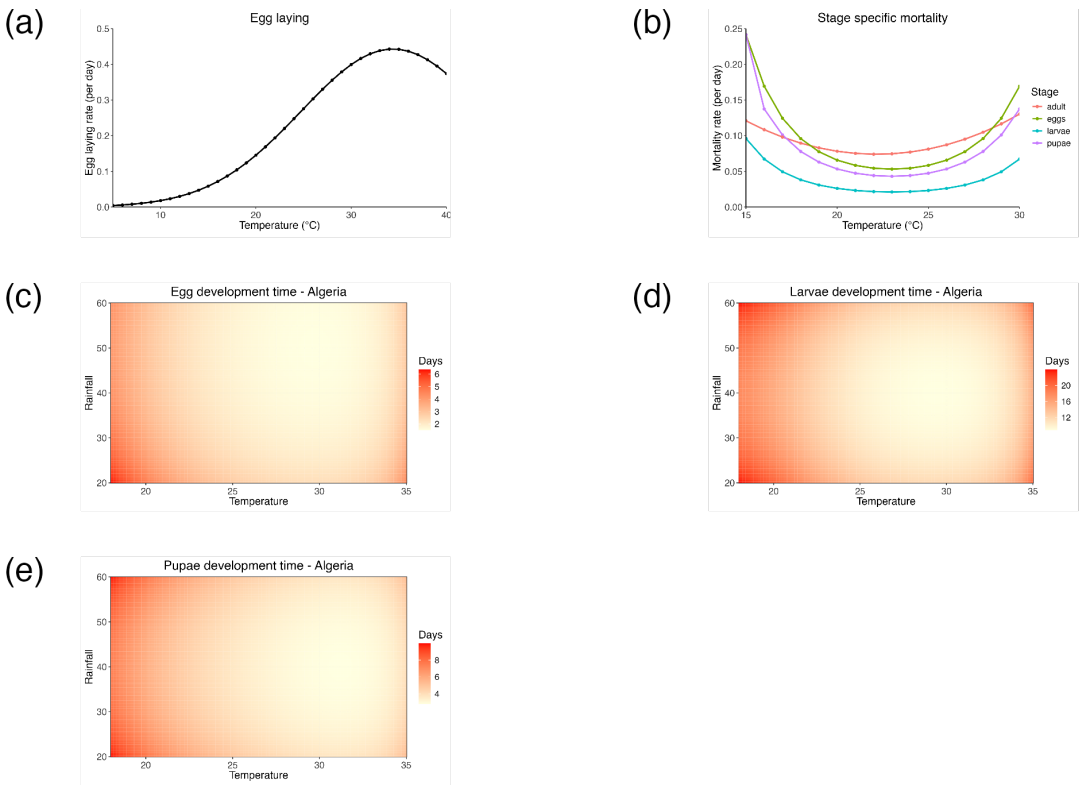

Figure 10: Functional relationships used to describe the relationship between life history parameters and weather variables including temperature and rainfall.

A.2.1 Temperature and rainfall

We assume that temperature and rainfall are seasonal and described by

$$T(t), R(t) = a + b_1 \sin\left(\frac{2\pi t}{365}\right) + b_2 \cos\left(\frac{2\pi t}{365}\right), \tag{A.2}$$

or

$$T(t), R(t) = T_0 \left[1 + T_1 \cos\left(\frac{2\pi}{365}(\omega t + \theta)\right)\right], \tag{A.3}$$

where a represent the mean ambient temperature near the surface of the water in degrees Celsius (°C). It also represent the mean of the cummulative rainfall in mm; b_1 and b_2 affect the magnitude and timing of annual temperature or cummulative rainfall in equation A.2. In equation A.3, T_0 is the mean annual temperature or cummulative rainfall, T_1 captures variations about the mean, w and θ represent the periodicity and phase shift of the function respectively [8, 16, 1, 4]. For each region, we determine the performance of the fitting by calculating the R^2 values and these are recorded in table 2. Temperature and rainfall data as shown in figure 2 are also recorded in table 3.

Table 2: R^2 values for function fittings to temperature and rainfall data across four African regions.

Region	Temperature (T(t))	Rainfall (R(t))
Ghana	0.97	0.62
Algeria	0.99	0.96
Kenya	0.90	0.64
South Africa	0.99	0.88

Table 3: Monthly Average Temperature and Rainfall in Four African Countries. Data is taken from World Weather Online. Sources to specific regions include [17], [18], [19], and [20].

	Ghana		**Algeria**		**Kenya**		**South Africa**	
Month	Temp (°C)	Rainfall (mm)	Temp (°C)	Rainfall (mm)	Temp (°C)	Rainfall (mm)	Temp (°C)	Rainfall (mm)
January	29	23.5	6.5	30.7	20	66.3	22	19.3
February	29.5	82.2	7.5	25.2	21	85.1	22.5	14.9
March	29.5	208.9	10.5	39.3	22	111.9	21	28.4
April	29	233.4	15	57.4	20.5	260	19	64.6
May	28	230.9	20	60.7	19	197.8	17	115
June	26.5	305.2	25.5	33.7	18.5	118.6	15	201.9
July	25	246.5	29.5	14.7	18	66.5	14	125
August	25	214.8	28.5	30.4	19	68.7	14	149.5
September	25	352	23.5	61.7	20.5	69.9	15.5	79.3
October	26.6	314.7	17.5	53.7	21	105.7	17	49.4
November	27.5	104.7	11.0	32.7	20	155.4	19	45.6
December	28	26.9	7.5	18.5	19	108.7	20.5	26.2

A.3 Numerical solution

The system of equations 2.1 were solved using the *deSolve* package in R. We use the ggplot2 package to produce visualization of the model outcomes. Parameter values used in solving the model is presented in table 4.

Table 4: Values and functions of the parameters of the model 2.1.

Parameter	**Range/Function Form**	**References**
b	[150, 300]	[1, 21]
δ_L	[0.02, 0.06]	[4]
ρ_{Ah}	[0.6, 2.3]	[2, 22]
ρ_{Ar}	[0.5, 1.5]	[22, 2]
K	$[500, 3 \times 10^6]$	[4, 11, 23]
$\phi_{Ao}(T)$	2.6	[12]
$\mu_E(T)$	2.4	[12, 10]
$\mu_L(T)$	2.4	[12, 10]
$\mu_P(T)$	2.4	[12, 10]
$\mu_A(T)$	2.5	[4, 10, 24]
$\rho_E(T, R)$	2.8	[10, 25, 1, 4]
$\rho_L(T, R)$	2.8	[10, 25, 1, 4]
$\rho_P(T, R)$	2.8	[10, 25, 1, 4]

References

[1] Ahmed Abdelrazec and Abba B Gumel. Mathematical assessment of the role of temperature and rainfall on mosquito population dynamics. In: *Journal of mathematical biology* 74.6 (2017), pp. 1351–1395.

[2] Priscilla Cailly et al. A climate-driven abundance model to assess mosquito control strategies. In: *Ecological Modelling* 227 (2012), pp. 7–17.

[3] Susan S Imbahale et al. A longitudinal study on Anopheles mosquito larval abundance in distinct geographical and environmental settings in western Kenya. In: *Malaria journal* 10.1 (2011), pp. 1–13.

[4] Kamaldeen Okuneye and Abba B Gumel. Analysis of a temperature-and rainfall-dependent model for malaria transmission dynamics. In: *Mathematical biosciences* 287 (2017), pp. 72–92.

[5] Krijn P Paaijmans et al. Relevant microclimate for determining the development rate of malaria mosquitoes and possible implications of climate change. In: *Malaria journal* 9 (2010), pp. 1–8.

[6] Krijn P Paaijmans et al. Unexpected high losses of Anopheles gambiae larvae due to rainfall. In: *PloS one* 2.11 (2007), e1146.

[7] EMILE Van Handel. Nutrient accumulation in three mosquitoes during larval development and its effect on young adults. In: *Journal of the American Mosquito Control Association* 4.3 (1988), pp. 374–376.

[8] Kamaldeen Okuneye, Ahmed Abdelrazec, and Abba B Gumel. Mathematical analysis of a weather-driven model for the population ecology of mosquitoes. In: *Mathematical Biosciences & Engineering* 15.1 (2018), pp. 57–93.

[9] Gbenga J Abiodun et al. Modelling the influence of temperature and rainfall on the population dynamics of Anopheles arabiensis. In: *Malaria journal* 15.1 (2016), pp. 1–15.

[10] Paul E Parham et al. Modeling the role of environmental variables on the population dynamics of the malaria vector Anopheles gambiae sensu stricto. In: *Malaria Journal* 11.1 (2012), pp. 1–13.

[11] FB Agusto, AB Gumel, and PE Parham. Qualitative assessment of the role of temperature variations on malaria transmission dynamics. In: *Journal of Biological Systems* 23.04 (2015), p. 1550030.

[12] Lindsay M Beck-Johnson et al. The effect of temperature on Anopheles mosquito population dynamics and the potential for malaria transmission. In: *PLOS one* 8.11 (2013), e79276.

[13] Mohamed Nabie Bayoh. Studies on the development and survival of Anopheles gambiae sensu stricto at various temperatures and relative humidities. PhD thesis. Durham University, 2001.

[14] Mohamed N Bayoh and Steve W Lindsay. Effect of temperature on the development of the aquatic stages of Anopheles gambiae sensu stricto (Diptera: Culicidae). In: *Bulletin of entomological research* 93.5 (2003), pp. 375–381.

[15] Mohamed N Bayoh and Steve W Lindsay. Temperature-related duration of aquatic stages of the Afrotropical malaria vector mosquito Anopheles gambiae in the laboratory. In: *Medical and veterinary entomology* 18.2 (2004), pp. 174–179.

[16] Amy Hurford, Xiunan Wang, and Xiao-Qiang Zhao. Regional climate affects salmon lice dynamics, stage structure and management. In: *Proceedings of the Royal Society B* 286.1904 (2019), p. 20190428.

[17] World Weather Online. *Kumasi Annual Weather Averages*. 2022. URL: https://www.worldweatheronline.com/kumasi-weather-averages/ashanti/gh.aspx (visited on 12/15/2022).

[18] World Weather Online. *Ain Mahbel Annual Weather Averages*. 2022. URL: https://www.worldweatheronline.com/ain-mahbel-weather-averages/ain-mahbel-area/al.aspx (visited on 12/15/2022).

[19] World Weather Online. *Cape Town Annual Weather Averages*. 2022. URL: https://www.worldweatheronline.com/nairobi-weather-averages/nairobi-area/ke.aspx (visited on 12/15/2022).

[20] World Weather Online. *Cape Town Annual Weather Averages*. 2022. URL: https://www.worldweatheronline.com/cape-town-weather-averages/western-cape/za.aspx (visited on 12/15/2022).

[21] Government of Canada. *Mosquitoes*. 2023. URL: https://www.canada.ca/en/health-canada/services/pest-control-tips/mosquitoes.html (visited on 03/10/2023).

[22] Theo H Jetten and Willem Takken. *Anophelism without malaria in Europe: a review of the ecology and distribution of the genus Anopheles in Europe*. 94-5. Wageningen Agricultural University, 1994.

[23] Franz Rubel et al. Explaining Usutu virus dynamics in Austria: model development and calibration. In: *Preventive veterinary medicine* 85.3-4 (2008), pp. 166–186.

[24] Erin A Mordecai et al. Detecting the impact of temperature on transmission of Zika, dengue, and chikungunya using mechanistic models. In: *PLoS neglected tropical diseases* 11.4 (2017), e0005568.

[25] Godwin Ray Anugboba Okogun et al. Life-table analysis of Anopheles malaria vectors: generational mortality as tool in mosquito vector abundance and control studies. In: *Journal of vector borne diseases* 42.2 (2005), p. 45.

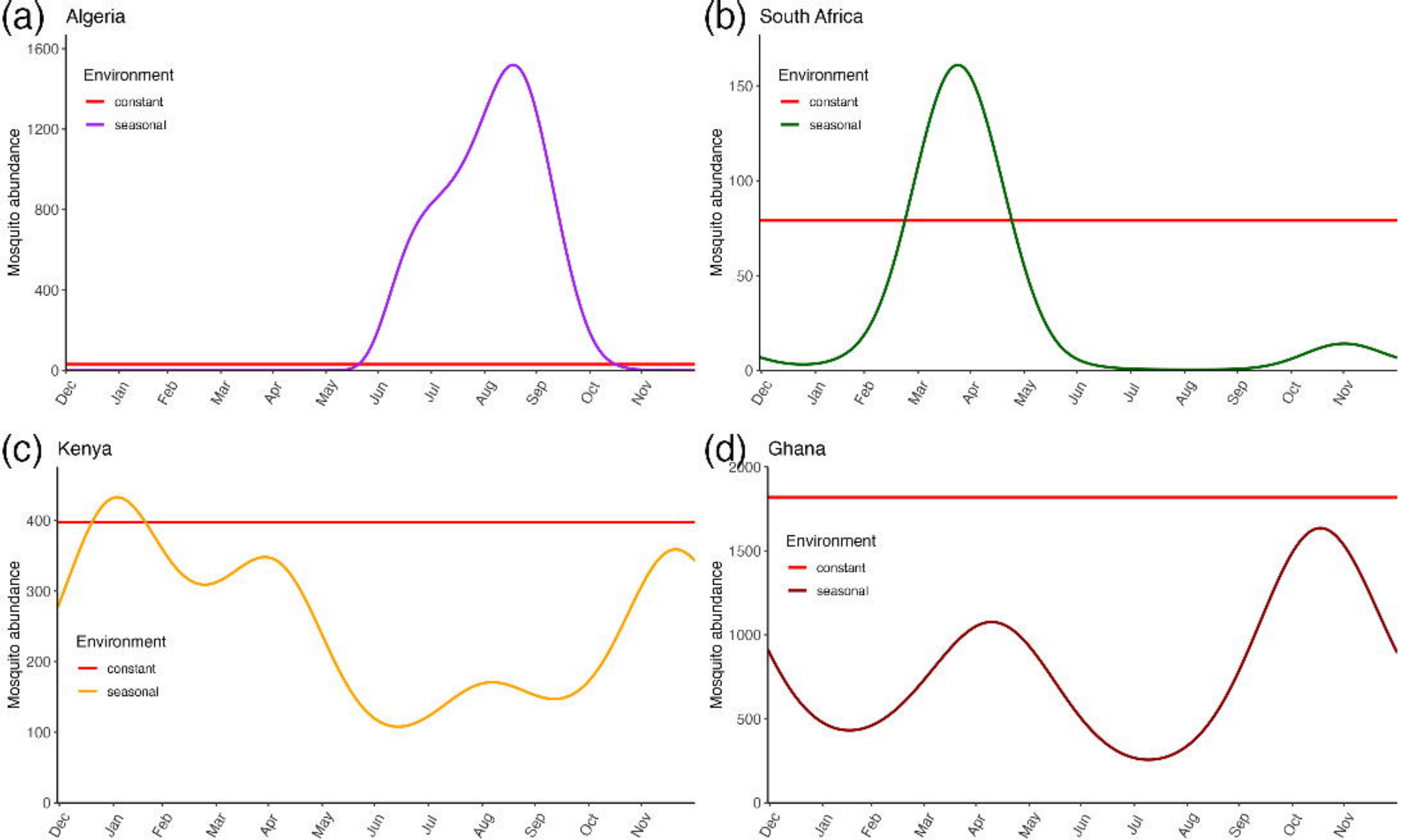
(a)
Algeria
Environment
constant
seasonal
Mosquito abundance
1600
1200
800
400
0
Dec
Jan
Feb
Mar
Apr
May
Jun
Jul
Aug
Sep
Oct
Nov
(b)
South Africa
Environment
constant
seasonal
Mosquito abundance
150
100
50
0
Dec
Jan
Feb
Mar
Apr
May
Jun
Jul
Aug
Sep
Oct
Nov
(c)
Kenya
Environment
constant
seasonal
Mosquito abundance
400
300
200
100
0
Dec
Jan
Feb
Mar
Apr
May
Jun
Jul
Aug
Sep
Oct
Nov
(d)
Ghana
Environment
constant
seasonal
Mosquito abundance
2000
1500
1000
500
0
Dec
Jan
Feb
Mar
Apr
May
Jun
Jul
Aug
Sep
Oct
Nov

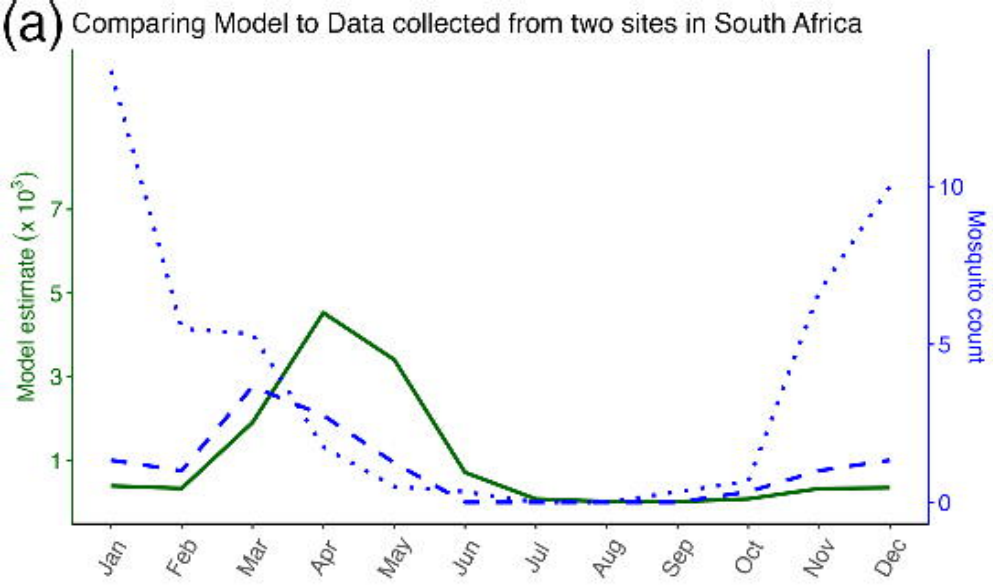
(a)
Comparing Model to Data collected from two sites in South Africa
Model estimate (x 10^3)
Mosquito count
Jan
Feb
Mar
Apr
May
Jun
Jul
Aug
Sep
Oct
Nov
Dec

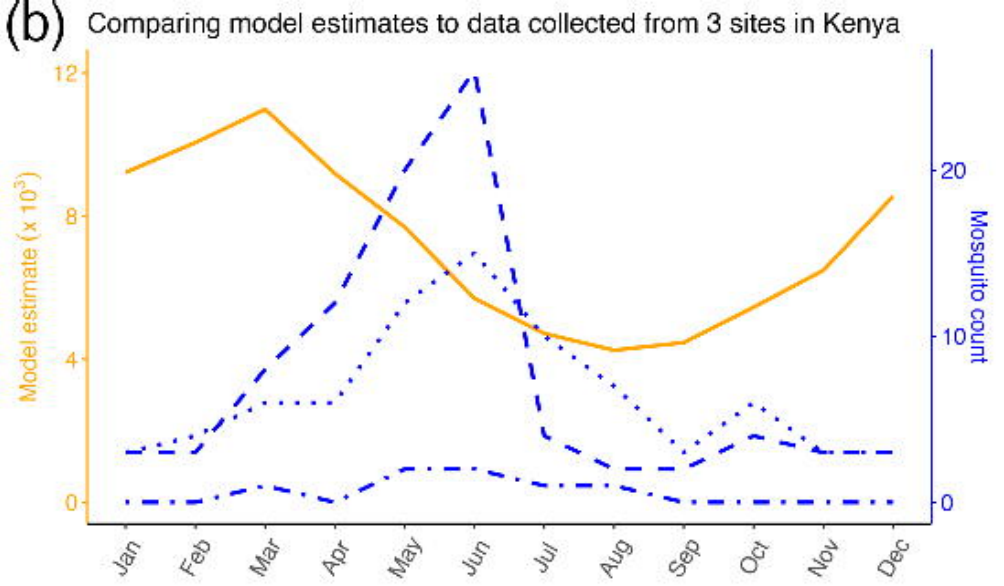
(b)
Comparing model estimates to data collected from 3 sites in Kenya
Model estimate (x 10^3)
Mosquito count
Jan
Feb
Mar
Apr
May
Jun
Jul
Aug
Sep
Oct
Nov
Dec

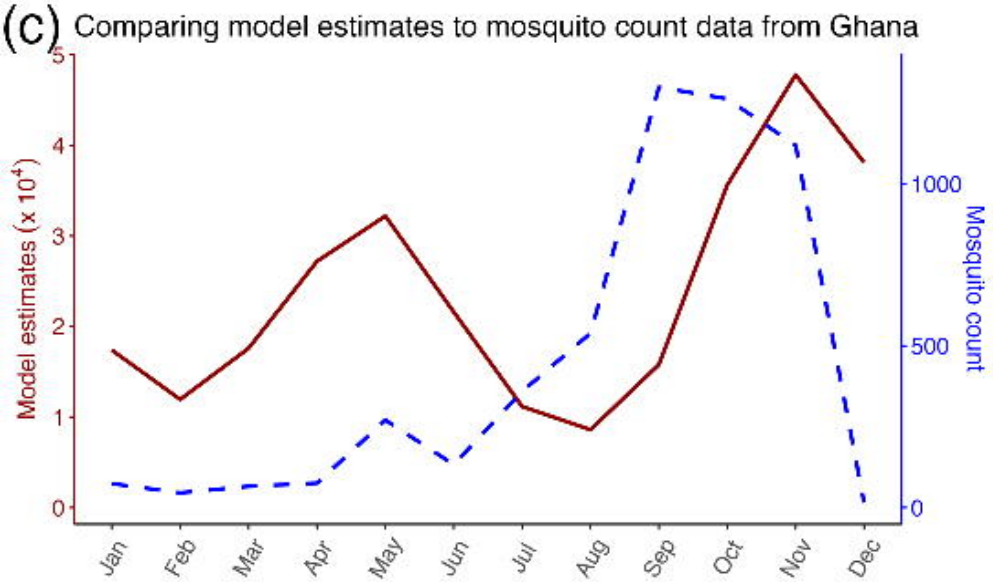
(c)
Comparing model estimates to mosquito count data from Ghana
Model estimates (x 10^4)
Mosquito count
Jan
Feb
Mar
Apr
May
Jun
Jul
Aug
Sep
Oct
Nov
Dec

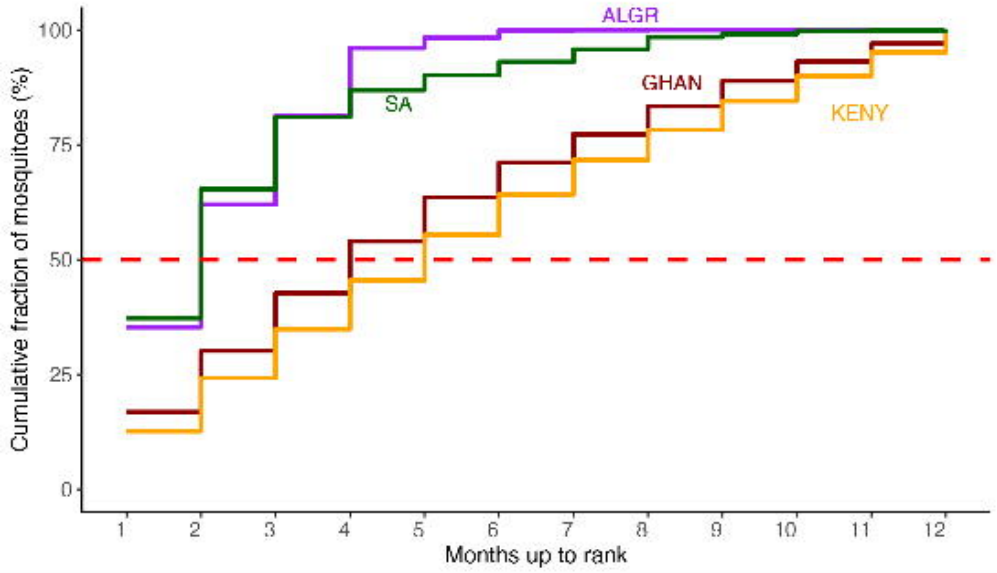
ALGR
SA
GHAN
KENY
Cumulative fraction of mosquitoes (%)
100
75
50
25
0
1
2
3
4
5
6
7
8
9
10
11
12
Months up to rank

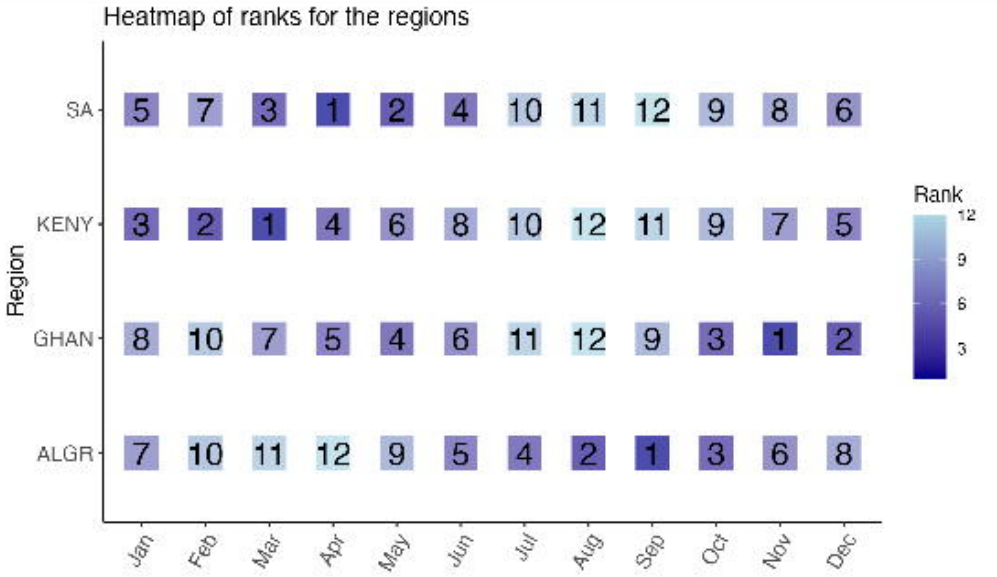
Heatmap of ranks for the regions
Region
SA
KENY
GHAN
ALGR
5 7 3 1 2 4 10 11 12 9 8 6
3 2 1 4 6 8 10 12 11 9 7 5
8 10 7 5 4 6 11 12 9 3 1 2
7 10 11 12 9 5 4 2 1 3 6 8
Jan
Feb
Mar
Apr
May
Jun
Jul
Aug
Sep
Oct
Nov
Dec
Rank
12
9
6
3

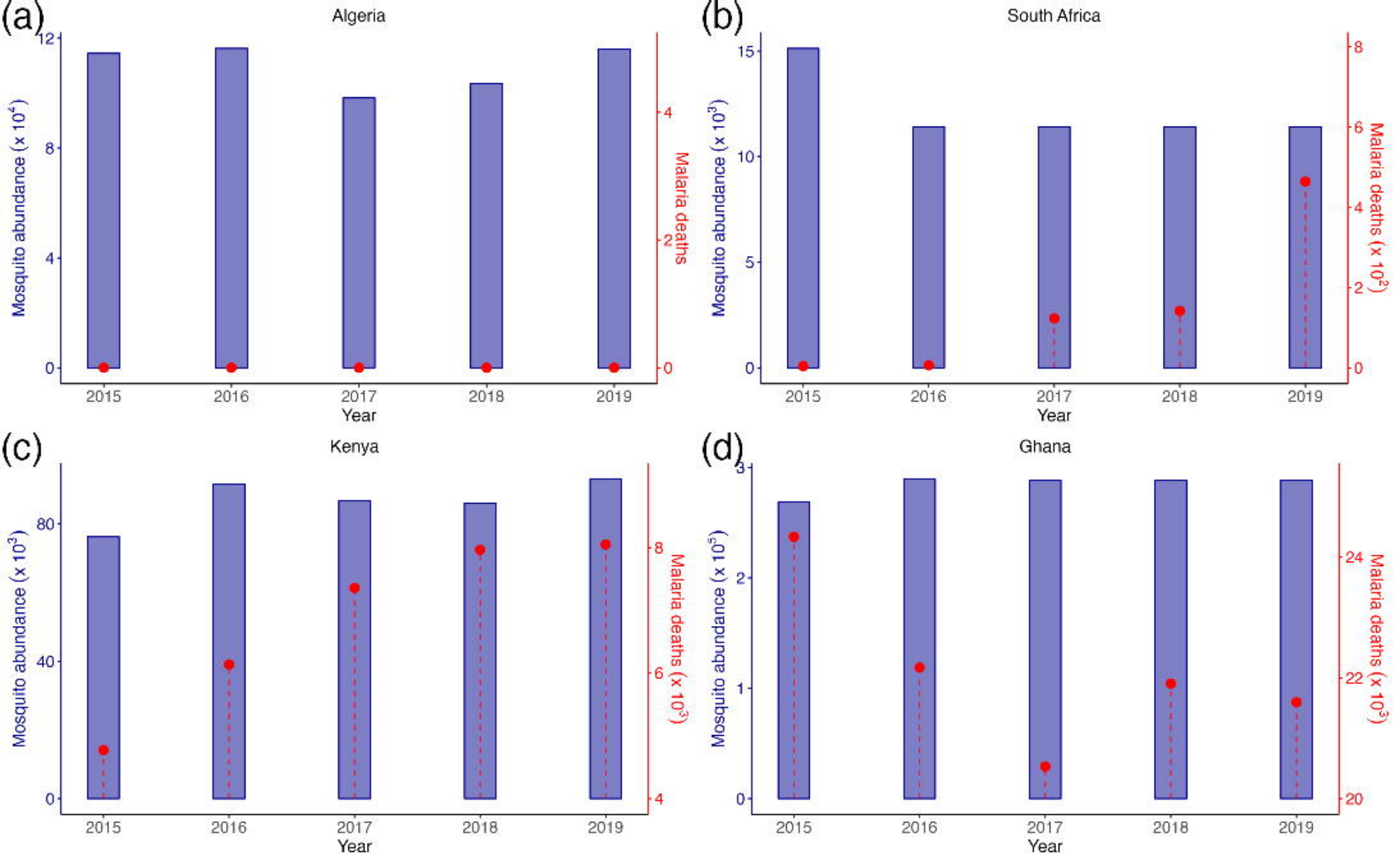
(a)
Algeria
Mosquito abundance (x 10^4)
Malaria deaths
Year
(b)
South Africa
Mosquito abundance (x 10^3)
Malaria deaths (x 10^2)
Year
(c)
Kenya
Mosquito abundance (x 10^3)
Malaria deaths (x 10^3)
Year
(d)
Ghana
Mosquito abundance (x 10^5)
Malaria deaths (x 10^3)
Year

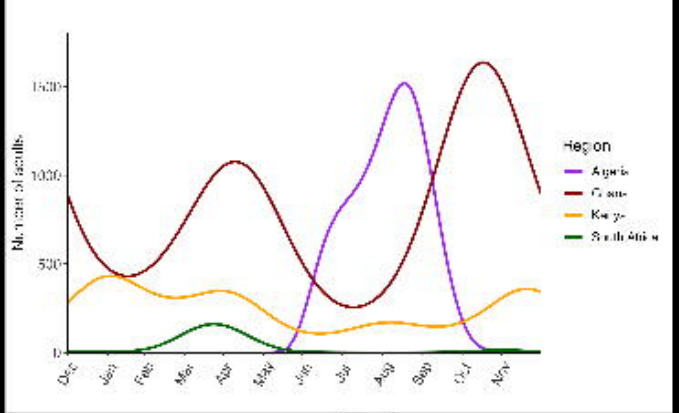
Region
Algeria
Ghana
Kenya
South Africa

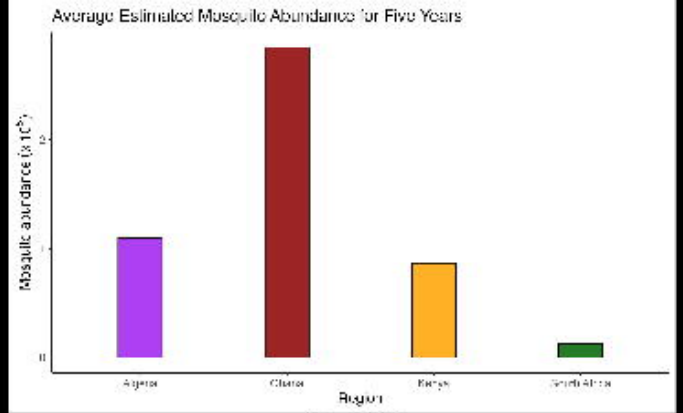
Average Estimated Mosquito Abundance for Five Years
Mosquito abundance
Region

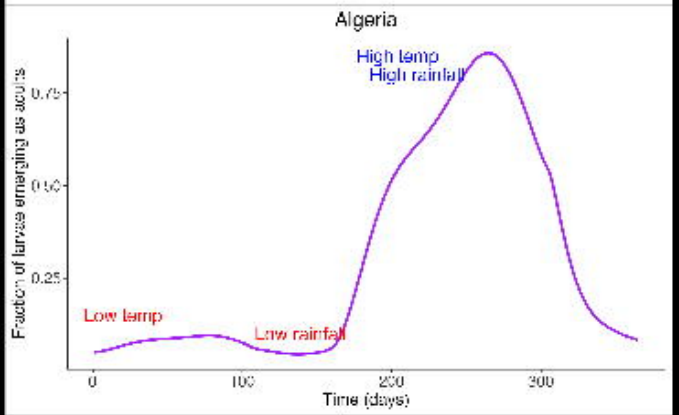
Algeria
High temp
High rainfall
Low temp
Low rainfall
Fraction of larvae emerging as adults
Time (days)

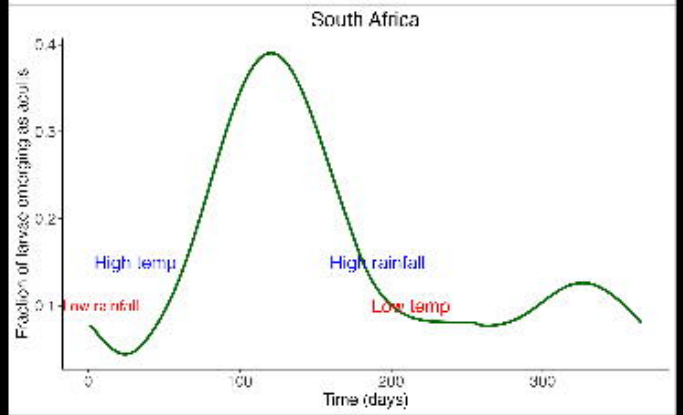
South Africa
High temp
High rainfall
Low rainfall
Low temp
Fraction of larvae emerging as adults
Time (days)

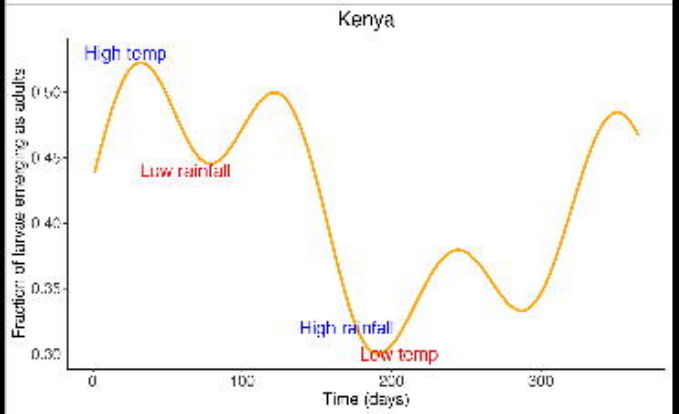
Kenya
High temp
Low rainfall
High rainfall
Low temp
Fraction of larvae emerging as adults
Time (days)

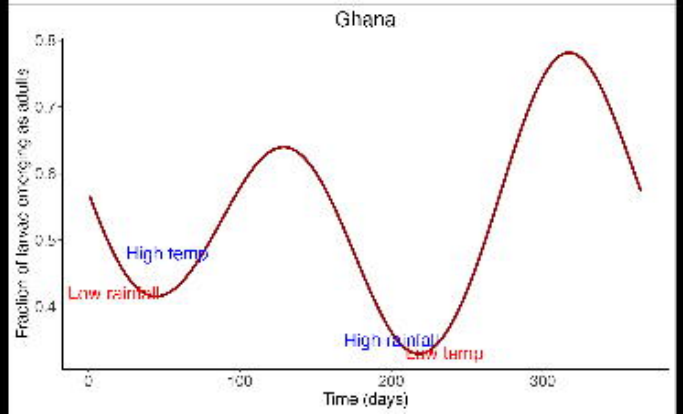
Ghana
High temp
Low rainfall
High rainfall
Low temp
Fraction of larvae emerging as adults
Time (days)

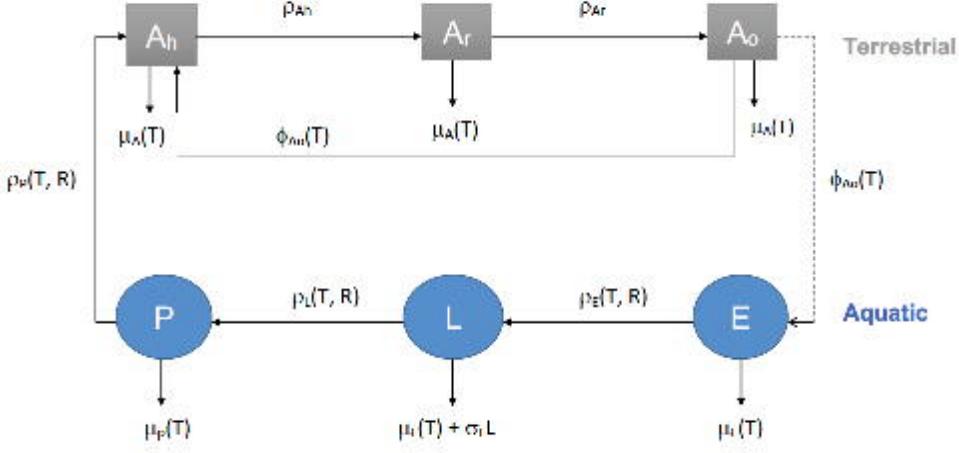
Ah
ρAh
Ar
ρAr
Ao
Terrestrial
μA(T)
ϕAm(T)
μA(T)
μA(T)
ρP(T, R)
ϕAm(T)
P
ρL(T, R)
L
ρE(T, R)
E
Aquatic
μP(T)
μL(T) + σL L
μE(T)

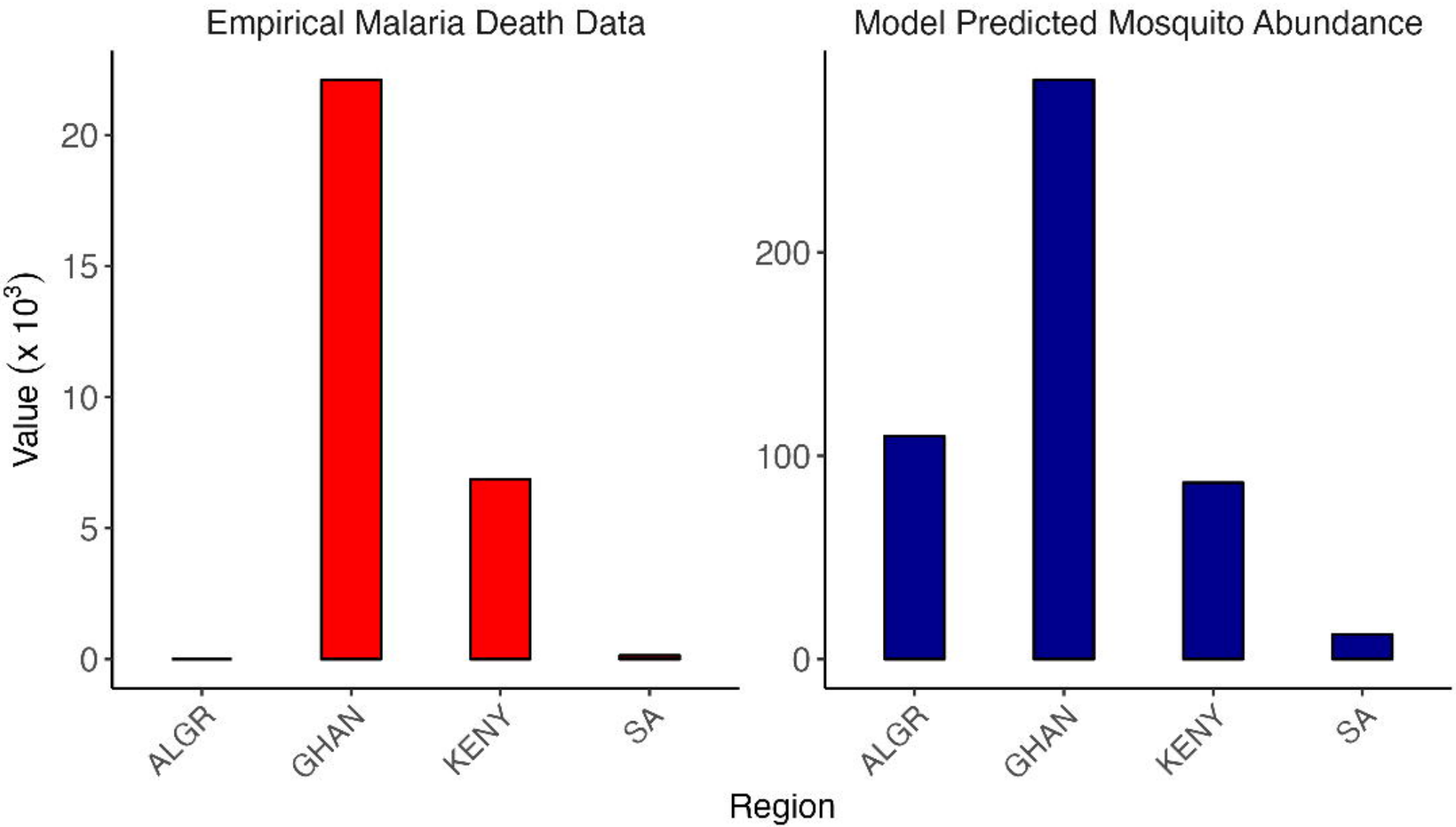
Empirical Malaria Death Data
Model Predicted Mosquito Abundance
Value (x 10^3)
0
5
10
15
20
0
100
200
ALGR
GHAN
KENY
SA
ALGR
GHAN
KENY
SA
Region

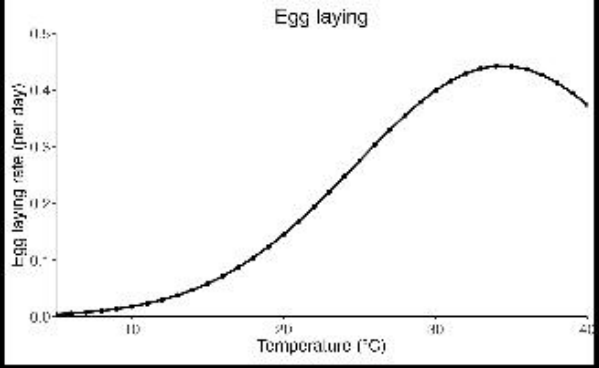
Egg laying
Egg laying rate (per day)
Temperature (°C)

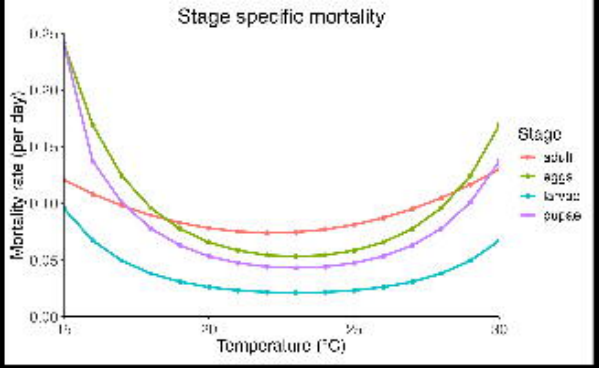
Stage specific mortality
Mortality rate (per day)
Temperature (°C)
Stage
adult
eggs
larvae
pupae

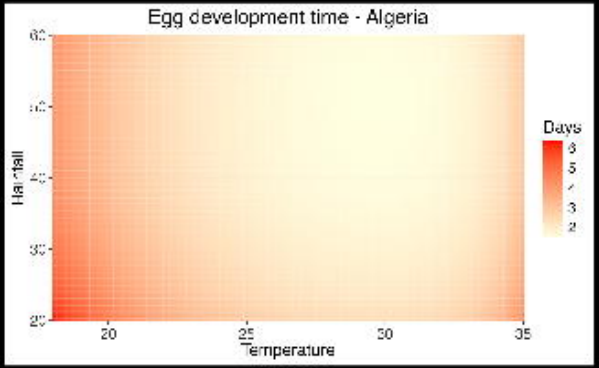
Egg development time - Algeria
Rainfall
Temperature
Days

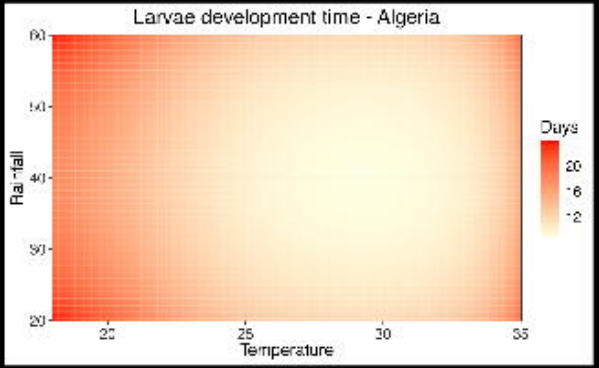
Larvae development time - Algeria
Rainfall
Temperature
Days

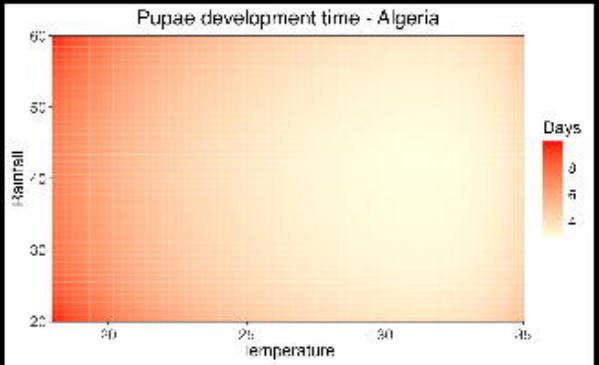
Pupae development time - Algeria
Rainfall
Temperature
Days

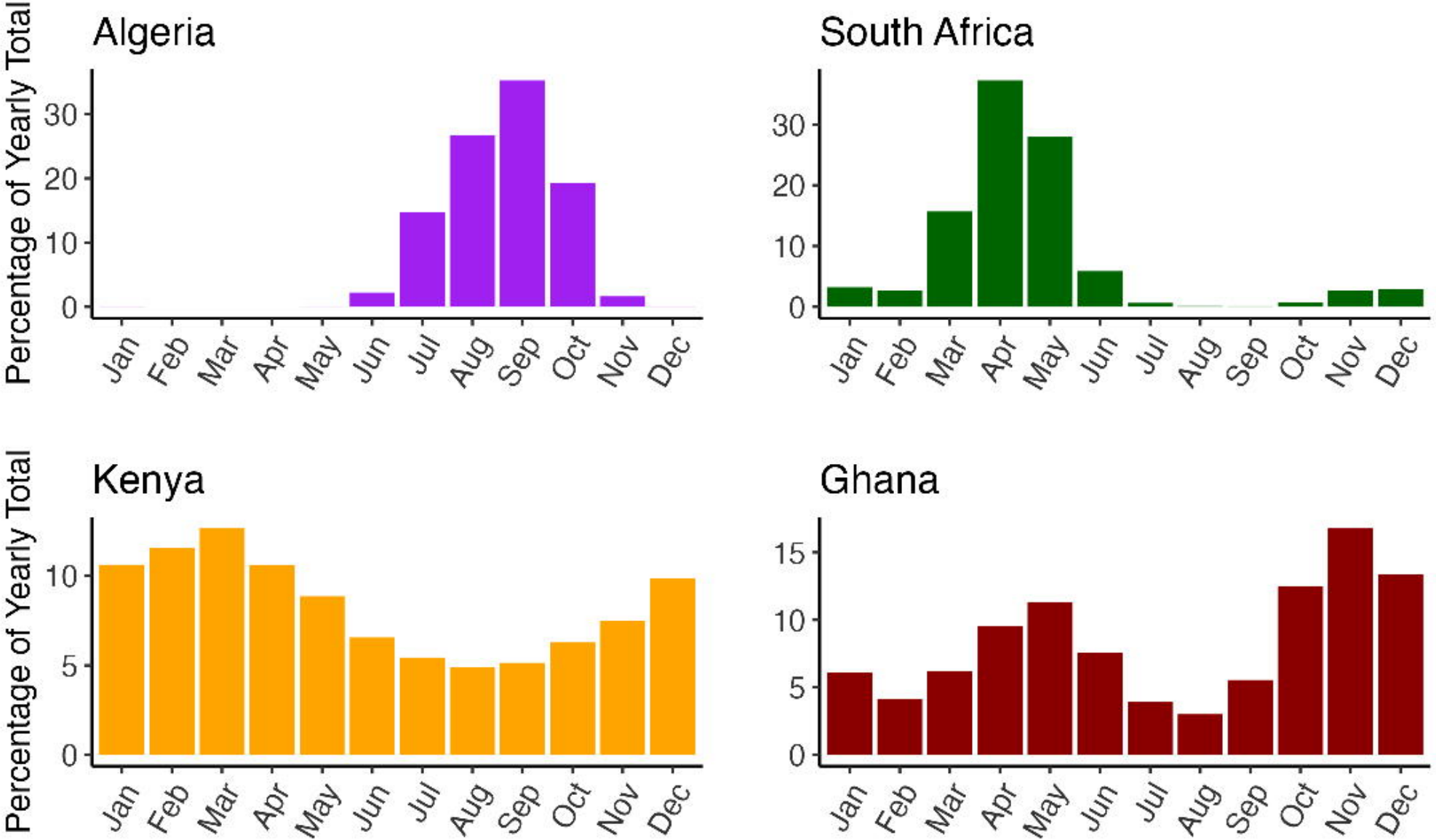
Algeria
South Africa
Kenya
Ghana
Percentage of Yearly Total
Percentage of Yearly Total
0
10
20
30
0
10
20
30
0
5
10
0
5
10
15
Jan
Feb
Mar
Apr
May
Jun
Jul
Aug
Sep
Oct
Nov
Dec

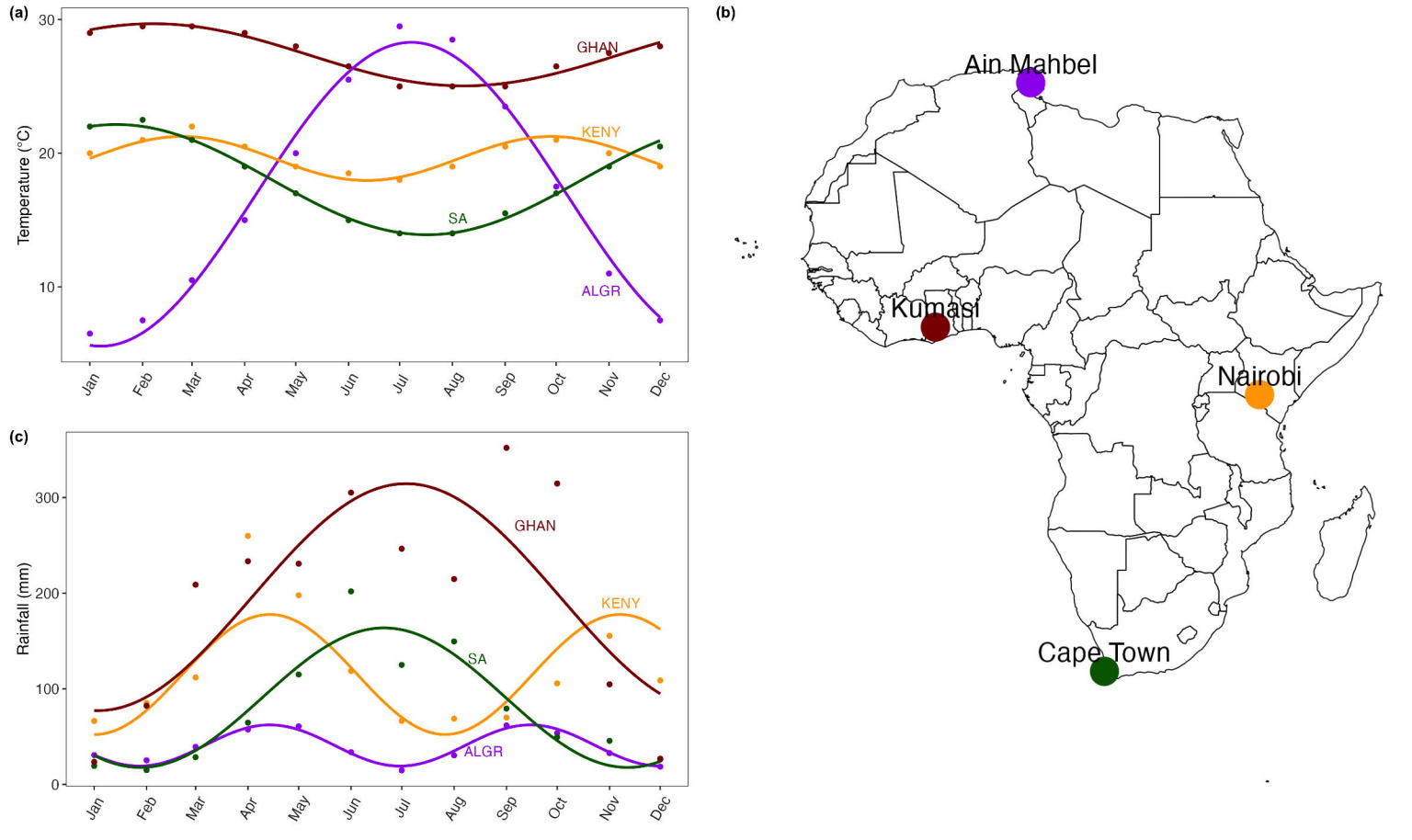
(a)
Temperature (°C)
30
20
10
GHAN
KENY
SA
ALGR
Jan
Feb
Mar
Apr
May
Jun
Jul
Aug
Sep
Oct
Nov
Dec
(b)
Ain Mahbel
Kumasi
Nairobi
Cape Town
(c)
Rainfall (mm)
300
200
100
0
GHAN
KENY
SA
ALGR
Jan
Feb
Mar
Apr
May
Jun
Jul
Aug
Sep
Oct
Nov
Dec